Kragujevac J. Sci. (2025) 47 (2) 59-88
doi: 10.5937/KgJSci2502059P

UDC 611.018.82:53.082.74:57.085
Original scientific paper

NEURAL RECONNECTION AFTER EXPOSURE IN HIGH FREQUENCY ELECTROMAGNETIC FIELDS - *IN VIVO* STUDY

Milan G Paraš[1], Dragana M Šnjegota[2], Zoran Nj Ružić[3], Maja R Šibarević[2], Jovana M Grahovac[2], Radoslav B Gajanin[4], Smiljana D Paraš*[2]

[1]*Faculty of Physics University of Vienna, 1180 Vienna, Austria*
[2]*Faculty of Natural Sciences and Mathematics University of Banja Luka, 78000 Banja Luka, Bosnia and Herzegovina*
[3]*Faculty of Agriculture, Department of Veterinary, University of Novi Sad, 21000 Novi Sad, Republic of Serbia*
[4]*Faculty of Medicine University of Banja Luka,78000 Banja Luka, Bosnia and Herzegovina*
*Corresponding author; E-mail: smiljana.paras@pmf.unibl.org

(Received January 15, 2025; Accepted April 10, 2025)

ABSTRACT: Change in cytoarchitecture and reconnection of neurons in rats' brain under direct two months high frequency electromagnetic field (HFEMF) exposure has been found, supported with data and discussed. HFEMF used in the experiment had the following characteristics: 2.0 GHz frequency, 0.015 A/m intensity, electric field strength of 5.64 V/m, and SAR value was 2.5 W/kg. Rats were exposed for 6 hours a day for 6 days a week, during period of 60 days with experimental HFEMF. Six months after the treatment, histological and unbiased stereological analyses show that there is a reconnection of neurons in rats´ brain, demonstrated by slight increase in their number and production of new dendrites. Effects of HFEMF on neuronal disconnection were detected via caspase, while the SNXS25 protein indicated their reconnection and regeneration. Immunohistochemical analysis of nervous tissue in this paper shows that HFEMF disrupt the work of proteins found on cell membranes and endocytic function of neurons and thus interrupts interneuron communication. The advantage of HFEMF over other methods of treating brain damage is in their controlled and very precise use, with specifically defined characteristics of HFEMF, without ionizing and mutagenic effect on neurons.

Key words: interneuron communication, Purkinje cells, stereological analysis, apoptosis, SNXS25 protein, TEM

INTRODUCTION

Function of nervous system is based on electrical and chemical signals between two or more neurons and between neurons and receptor or effector cells (MAC VICAR and THOMPSON, 2010). Electrical signalling occurs through two main mechanisms: one involves pathways of low resistance between neighbouring neurons that are provided by intercellular channels

ORCID:
D. Šnjegota - 0000-0003-2125-4635; Z. Ružić - 0000-0001-7754-7264; M. Šibarević - 0009-0007-2910-2501; R. Gajanin - 0000-0002-9760-9829; S. Paraš - 0000-0001-8617-3583.

(SHENG *et al.,* 2012). Second pathways occur as a consequence of the extracellular electrical fields generated by neurons during electrical signalling (BERZHANSKAYA *et al.,* 2013; HAN *et al.,* 2018). It has been proven that electric fields have an excitatory effect on neurons, increase their plasticity and have facilitators that stimulate neuroregeneration (FABER and PEREDA, 2018; NAGAPPAN *et al.,* 2020). The study of mechanisms of rupture due to HFEMF (high frequency electromagnetic fields) and the re-establishment (reconnection) of synapses between neurons is very important in order to regenerate the nerve tissue (KIVRAK *et al.,* 2017; ZANDI-MEHRAN *et al.,* 2020).

Processes of altered transduction of electrical and chemical signals interfere with the neurons of the central system to communicate with each other in order to respond to physiological stimuli (FLØNES *et al.,* 2018; LAU *et al.,* 2020). After exposure to HFEMFs, pyramidal neurons have pyknotic nuclei, separated from each other, lost their properly arranged spatial arrangement in the pyramidal layer of the rat hippocampus and the connection between them and neurites has weakened (EL-KAFOURY *et al.,* 2019). Some authors imply that even LFEMFs (low frequency electromagnetic field) disrupted communication between neurons and neurites (ZHENG *et al.,* 2017). At the molecular level EMFs stimulated the signalling of inflammatory cells and increased proliferation and differentiation of endogenous mesenchyme stem cells (ROSS *et al.,* 2017). EMFs allowed for stronger infiltration of peripheral circulating macrophages among nerve cells to phagocytize damaged axonal and other neuronal debris (TEIMORI *et al.,* 2017). Induced apoptosis in nervous tissue with HFEMF leads to a decrease in the number and disconnection of neurons. In the cerebellum of rats, there is a decrease in the number of Purkinje cells after exposure to 0.9 GHz HFEMF (SONMEZ *et al.,* 2010). In the work of ERTILAV *et al.* (2018) suggested that the HFEMF frequencies of from 0.9 to 1.8 GHz led to modulation of molecular pathways on cell membranes, increased levels of apoptosis and caspase activation in rat neurons. In addition, these HFEMFs lead to excessive influx of calcium ions into neurons (ERTILAV *et al.,* 2018). In work of VARGHESE et al. (2018) shows that in female rats exposed to 2.45 GHz HFEMF, a quantitative increase in caspase 3 markers on neurons also occurred. In addition, there was a decrease in dendritic branches, absorption of dendritic neurons, changes in the structure of dendrites and a decrease in neuronal signalling (VARGHESE *et al.,* 2018).

The regeneration of interneuronal communication and the increase in neuronal endocytosis function are detected through sorting nexin proteins (SNXS) in cell membranes and cytoplasm of neurons (TEASDALE and COLLINS, 2012; DU *et al.,* 2013; TAKEMURA *et al.,* 2020a; OTTO and THUMM, 2020; TAKEMURA *et al.,* 2020b). Therefore, SNXN proteins were selected as markers for detecting the regeneration process in our study. In work of MESENTIER-LOURO *et al.* (2019) shows an increase in the activity of hippocampal neurons in mice with neurodegenerative diseases across SNXS proteins. The main mechanism that enables regeneration of neurons is stimulation and cessation of inhibition of their damaged synaptic membranes (MESENTIER-LOURO *et al.,* 2019). Neuroregeneration involves reconnecting damaged nerve, its functioning and growth in order to be able to re-establish the flow of information through the damaged tissue (RONCAL *et al.,* 2019). After the connection, the damaged nerves must be stimulated in order to start transmitting signals, and this is mostly done with electricity (FARRUKH *et al.,* 2018).

MATERIALS AND METHODS

Characteristics of the High frequency electromagnetic field used in experiment

HFEMF used in the experiment had the following characteristics: 2.0 GHz frequency, 0.015 A/m intensity and electric field strength of 5.64 V/m. SAR (specific absorption rate) value was of 2.5 W/kg per unit mass by whole rat body and measured with apparatus EN 50361:2001

(Emitech). HFEMF used by the authors in this study were the same during every day of treatment and were controlled. Authors decided these characteristics and protocol of HFEMF because they are increasingly present in the human environment. External HFEMFs of the surrounding environment were also present but were neglected due to the inability to control them. The strength of the HFEMF that were used in experiment was measured by „PROTECT" Ltd, rapport date December 22, 2019, and time 11:00, air temperature at the moment of HFEMF intensity measurement was 5 ºC. The equipment used for fields´ strength measurement was HF 6080 Rev2 No.01099, Hyper LOG 6080, manufactured by AARONIA Germany. The instrument frequency and measurement range were 1-7 GHz, 10-90 dBm, antenna 0.68-6 GHz, manufactured in 2018 year.

Experimental protocol

All animal procedure were in compliance with Directive 2010/63/EU on the protection of animals used for experimental and other scientific purposes and were approved by the University of Banja Luka Ethical Committee on Animal Experiments, permission number No. 01-9-192.2/19. The experiment was performed on 45 males sexually mature Wistar rats (*Ratus norvegicus*), at the age of 8 weeks, and body weight 220-250 g. Animals were placed in individual Plexiglas cages (dimensions of cage were 30x45x25 cm), three rats per one cage. During the experiment, the animals were kept under following conditions: temperature 23±3 ºC, air humidity 55±5%, 6-10 air changes/h, and artificial lighting at intervals of 12 h day/night. The animals had free access to food and water. A veterinarian, trained working with experimental vertebrates, was daily monitored animal health (certificate No. 24-2/2018, Ministry of Agriculture, Forestry and Water Management). No deaths rats were recorded during the experiment. Rats were divided randomly into three groups at the vivarium. One group (control group) of 15 rats was not exposed to any measurable experimental HFEMF; second group (exposured group) of 15 rats was exposed to experimental HFEMF for two months; and third group (regenerated group) of 15 rats was exposed with experimental HFEMF for two months and then after that period rats stayed for another six months in conditions without exposure to the fields. Mobile communication antenna Alpha 41 (Siretta, Enabling Industrial IoT) was the source of HFEMF with overall frequency coverage from 1.7 to 2.7 GHz in experiment. The antenna was with flexible horizontal and vertical polarization plane. Exposure and regenerated groups were exposed 6 hours a day (from 09:00 to 15:00h) for 6 days a week during 60 days with experimental HFEMF. Antenna Alpha 41 was 5 cm away from the rat cage. Rats were exposed to HFEMF in one area of the laboratory in their cages. The fields were distributed evenly over the whole cage surface during exposure of rats. After exposure rats from exposed and regenerated group were brought to the room where control rats were staying. After exposure rats from regenerated group were brought to the room where the control rats were staying. After completion of the exposure treatment, regenerated group remained for another two months under the same laboratory conditions as control group.

Haematological analysis

At the end of the experimental treatment for each group of rats, blood samples were taken from the right ventricle of heart of all rats for haematological analysis. All blood samplings from the rats were performed under anaesthesia (Ketamine 90 mg/kg body weight. Ketamine Hydrochloride Injection USP Rotexmedica-Germany in combination with Xylazine 5 mg/kg body weight 2% Xylazine, Cp Pharm, Bergdorf, Germany) and effort were made to minimize the suffering of the animals. Blood for analysis, average 5 ml, was decanted and centrifuged at 10000 rpm. All haematological and blood biochemical parameters were measured using the automatic haematological analyser (Roche, Cobas Integra 400). Parameters of haematological analysis were: number of red blood cells (RBC), mean erythrocytes´ volume

(MCV), mean erythrocytes´ haemoglobin (MCH), mean corpuscular haemoglobin concentration (MCHC), red blood cells distribution (RCD), haemoglobin (HG), haematocrit (HC), white blood cells (WBC), lymphocytes (LYM), monocytes (MON), granulocytes (NEUT-neutrophil, EOS-eosinophil, BAS-basophil), platelet count (PLC), mean platelet volume (PLV). Parameters of blood biochemical analysis were: total protein, triglycerides, cholesterol, glucose, creatinine, total bilirubin, alkaline phosphatase, aspartate amino transferase (AST), alanine amino transferase (ALT), glutamate pyruvate transferase (GPT), gamma glutamate transferase (GGT), pancreas lipase, urea, potassium, sodium and calcium.

Histological and stereological analysis

After the sixty days of control and exposure group and 240 days of regenerated group all experimental treatments 45 rats were decapitated. The rats' brain (cerebrum and cerebellum) was removed, immersed in Bouin's solution for 24 h, for better adsorption, further cut into smaller parts and then immersed into fresh Bouin's solution. Subsequently, all of the dissected brains were prepared for light microscopy using the standard tissue preparation procedure. Samples of tissue of all brains was embedded in paraffin and were cut in a frontal plane on a Leica rotary Microtome RM 2165 (Leica Microsystems, Wetzlar, Germany), in 5 μm thick serial sections. Slices of all tissue were stained with Haematoxylin-Eosin (HE), Mallory-Azan trichrome, Toluidine blue and Crazy-violet stain (all stains by Merck KGaA, Darmstadt, Germany). The qualitative histology analysis of the brain's tissue slides was performed while using the light microscope a Leica DM8000 microscope with a MEGA VIEW camera and software system for digital image transfer (Wetzlar, Germany), and magnification of 20X, 50X, 100X, 250X and 400X. For quantitative, stereological analysis, micrographs of the brain's tissue were acquired in the RGB layout and converted to binary format. Measurements were made using a stereo-universal test system according to Cavalier's principle, with using 16.0 point-counting system (MBF software system Application Suite 3.0.0., MBF Bioscience, Williston, VT, USA), with P2 spacing grid at the maximum 400X magnification. Stereological measurement procedure is the same as in author's work PARAŠ et al., 2020 are applied in our work (PARAŠ *et al.,* 2020). Stained tissue sections of brains were used to measure the number and volume density (Vv) of their neurons and capillary endothelial cells through the following formula: Vv=Pf/Pt (mm^0) (NESTOROVIĆ *et al.,* 2016) and numerical density (Nv) (1) (SANTOS *et al.,* 2009):

$$Nv=\frac{Q}{Vo}=\frac{Q}{\sum_{i=1}^{n} Pi\times a\times h}\ (mm^{-3}) \qquad (1)$$

MBF software system was used to measure the surface and volume of all neurons and their nuclei, by the thickness of their diameters. The ratio between the neurons' nuclei and cytoplasm volume was used to determine the nucleocytoplasmic ratio (NCR). The mitotic index was determined at the ratio between the number of neurones in mitosis and the total number of neurons in 10 visible optical fields per slide, with maximum 200X magnification. The apoptotic index was determined at the ratio between the number of neurons in apoptosis and the total number of neurons in 10 visible optical fields per slide, with maximum 200X magnification (PARAŠ *et al.,* 2020).

Immunohistochemical analysis

The samples of brains tissue were used for immunohistochemical analysis of neuronal apoptosis and regeneration. Neurons detection in apoptosis was performed via caspase-3 expression, while neuron detection in regeneration was performed via SNXS25 protein expression. The procedures for expression caspase-3 and SNXS25 were performed according

to the manufacturer's instructions by Roche Diagnostics GmbH. The caspasa-3 staining method was employed to detect neurons apoptosis. Rabbit anti-rat caspase-3 immunohistochemistry kits were employed to detect the expression of the protein. Analysis system was used to calculate the total number of positive neurons the cortical and medulla area of cerebrum and cerebellum (LIU *et al.,* 2013). The samples of brain incubated with rabbit IgG against SNXS25 for 72 h at 4 °C and primary antibodies were probed with anti-rabbit IgG antibody labelled with peroxidase for 1 h at 25 °C. The sites of peroxidase were visualized with diaminobenzidine containing nickel-chloride. To establish a control, some sections were incubated with rabbit IgG against SNXS25 that had been pre-adsorbed overnight at 4 °C with recombinant SNXS25 protein (all immunohistochemical methods and techniques were by DAKO LSAB^{+}/HRP and Roche Diagnostics GmbH, Germany). Following immunohistochemistry methods, the sections of brain tissue were examined under a light microscope to observe apoptotic and regenerated neurons in rats' cerebrum and cerebellum.

Ultrastructural analysis

Representative parts of all isolated brains of rats from both experimental and control groups were cut under stereomicroscope into 1x1 mm samples. Ten samples were taken from each brain and first fixed for 0.5-1 min in Harrewald's solution. Then samples were transferred to a 2.5% glutaraldehyde solution in 0.1 M phosphate buffer (pH 7.2), and after 3 minutes, this solution was replaced with a new glutaraldehyde solution. Next, these samples were replaced to ethanol and acetone, and they were embedded into epoxy resin. The ultra-thin section obtained by ultramicrotome Leica EM UC6 (Leica, Germany), was studied using Transmission Electron Microscopy (TEM) Zeiss EM902 at the high voltage of 80.0 kV. The ultra-thin section was looked through first at a light microscope with small magnification 500X, and then the selected sections were more carefully studied under higher magnifications in the range of 12000-28000X.

Statistical analysis

All of the measured value results were presented as mean ± standard deviation. Group comparisons were performed while using parametric (two-way ANOVA, one-way ANOVA followed with Dunnett's test and t-test) or non-parametric tests (Kruskal-Wallis and Mann-Whitney U-test), depending on data distribution, with significance set at $p<0.05$. Statistical software SPSS 20.0 (IMB corp., Armonk, NY, USA) was used for data processing.

RESULTS

Haematological

Influence of HFEMF led to changes in the values of haematological parameters of rats' exposure group in relation to the control. In our study, there was a return to the value of the number and percentage of blood elements, and thus the dynamism of the blood in the regenerated group as they were in the control group of rats (Tab. 1). In general, all haematological parameters of the exposure group of rats had increased values, except for monocytes, eosinophil and basophils, whose value decreased. Statistically significantly increased values of white blood cells ($p=0.0152$), lymphocytes ($p=0.0211$), while significantly decreased values of monocytes ($p=0.0125$), the percentage of monocytes of WBC ($p=0.0167$), eosinophil ($p=0.0233$) and the percentage of eosinophil ($p=0.0257$) of the WBC exposure group relative to the control. In the regenerated group, the values of most of the haematological parameters of rats decreased in relation to the exposure group and their return to values very similar to the control group. The mean values of all determined parameters for all three

experimental groups of rats do not go beyond the reference values (SASSE, 1995; GIKNIS and CLIFFORD, 2012).

Table 1. Results of rat blood analysis in control and both experimental groups; value are shows as mean ± SD (*p<0.05, Dunnett's test)

Parameters	Control group (n=15)	Exposured group (n=15)	Regenerated group (n=15)	Reference range
Red blood cells (10^6/mm^3)	8.37±1.44	9.47±1.59	8.42±1.48	7.27-9.65
Mean cell volume (μm^3)	47.25±2.12	56.95±2.24	48.35±2.33	48.9-57.9
Mean cell hemoglobin (pg)	17.14±2.38	20.16±3.16	17.28±2.32	17.1-20.4
Mean corpuscular hemoglobin concentration (g/dl)	35.64±2.68	37.15±2.76	36.85±2.89	29.9-37.5
Red blood cells distribution width (%)	16.09±1.35	16.65±1.95	16.45±1.62	11.1-18.2
Hemoglobin (g/dl)	14.23±2.01	16.75±2.34	14.54±2.09	13.7-17.6
Hematocrit (%)	46.17±4.31	50.85±4.25	46.93±4.11	39.6-52.5
White blood cells (10^3/mm^3)	5.45±1.09	10.25±2.25*	6.04±1.12	1.96-8.25
Lymphocytes (10^3/mm^3)	4.15±1.04	7.92±1.45*	4.68±1.05	1.41-7.11
% lymphocytes of WBC (%)	76.15±7.45	77.27±8.03	77.48±7.38	55.6-86.3
Monocytes (10^3/mm^3)	0.16±0.09	0.08±0.07*	0.14±0.09	0.03-0.18
% monocytes of WBC (%)	2.94±0.27	0.8±0.16*	2.32±0.19	0.8-3.8
Neutrophil granulocytes (10^3/mm^3)	1.06±0.09	2.22±0.11	1.12±0.08	0.22-1.57
% neutrophil granulocytes of WBC (%)	19.45±3.44	21.63±3.85	18.54±3.75	6.2-26.7
Eosinophil granulocytes (10^3/mm^3)	0.06±0.01	0.02±0.01*	0.07±0.01	0.01-0.16
% eosinophil granulocytes of WBC (%)	1.09±0.02	0.20±0.03*	1.16±0.02	0.2-3.5
Basophil granulocytes (10^3/mm^3)	0.022±0.002	0.011±0.001	0.022±0.002	0-0.05
% basophil granulocytes of WBC (%)	0.37±0.09	0.10±0.04	0.50±0.08	0-0.8
Platelet count (10^3/mm^3)	672.32±78.45	694.66±69.14	669.42±74.33	538-1177
Mean platelet volume (μm^3)	8.85±1.85	8.91±2.06	8.89±1.99	6.2-9.4

Biochemical analysis of blood

Biochemical parameters indicate proper metabolism and blood supply to the organs of rats exposed to HFEMF (Tab. 2). Most of the analysed biochemical parameters of blood in exposed groups of rats had increased values. Statistically significantly increased values: triglycerides (p=0.0392), creatinin (p=0.0257), glucose (p=0.0412), aspartate amino transferase (p=0.0319) and pancreas lipase (p=0.0185) in the group of exposed rats compared to control group. The value of alkaline phosphatase was statistically significantly reduced (p=0.0284). In the regenerated group, the values of blood biochemical parameters return to very similar to the control group, except in the case of urea and glutamate pyruvate transfers whose value remains elevated. Mean values of all electrolytes (potassium, sodium and calcium) decreased in the

blood of rats from the exposure group compared to rats from the control group. In the regenerated group, the mean electrolyte values did not return to the values from the control group. It is important to note that the mean values of all parameters for all three groups of rats do not go beyond the reference values (SASSE, 1995; GIKNIS and CLIFFORD, 2012).

Table 2. Results of biochemical analysis of rat blood in control and both experimental groups; the values are shows as mean ± SD (*p< 0.05; Dunnett's test)

Parameters	Control group (n=15)	Exposured group (n=15)	Regenerated group (n=15)	Reference range
Total protein (mg/dL)	5.44±0.95	7.02±2.16	5.83±1.18	5.2-7.1
Triglycerides - mg/dL	21.77±3.15	46.25±4.06*	26.49±3.33	8.7-60.7
Cholesterol mg/dL	53.55±2.32	57.48±2.28	61.39±2.86	14.4-87.6
Glucose- mg/dl	110.41±8.51	197.25±9,02*	116.53±8.19	62.4-201.8
Creatinin- mg/dl	0.22±0.09	0.48±0.12*	0.31±0.09	0.2-0.5
Total Bilirubin - mg/dl	0.09±0.01	0.11±0.01	0.08±0.01	0.05-0.15
Alkaline Phosphatase - U/l	179.18±9.92	99.14±8.21*	165.55±9.58	62-230
Aspartate Aminotransferase - U/l	81.31±7.34	139.12±11.12*	95.44±9.83	74-143
Alanine Aminotransferase - U/l	24.44±2.07	28.15±2.22	27.61±2.17	18-45
Glutamate Piruvate Transferase - U/l	38.45±3.65	40.22±3.94	41.16±3.28	24-55
Gama Glutamate Transferase - U/l	4.54±0.61	6.39±0.59	4.02±0.94	2-12
Pancreas Lipase - mmol/l	4.55±2.39	10.16±3.09*	7.81±2.51	1-17
Urea - mmol/l	10.27±0.93	15.66±1.19	15.12±2.14	12.3-24.6
Potassium - mmol/l	3.99±0.45	2.05±0.52	2.74±0.48	3.82-5.55
Sodium – mmol/l	149.22±10.12	124.96±15.33	131.41±12.74	164.25-110.15
Calcium – mmol/l	1.35±0.09	1.14±0.09	1.21±0.11	1.05-2.34

Histological and stereological analysis of cerebellum tissue

Application of stereological unbiased measurements of the cross-section of cerebellum tissue enabled the quantitative detection of changes in its histological and cytological structure (Tab. 3).

Table 3. Stereological parameters of cerebellum tissue in control and both experimental groups of rats, value are shown as mean ± SD (*p<0.05; t-test)

Parameters	Control group (n=15)	Exposured group (n=15)	Regenerated group (n=15)
Volume density of stratum moleculare (mm^0)	0.368±0.088	0.342±0.037	0.352±0.055
Volume density of stratum gangliosum (mm^0)	0.099±0.011	0.052±0.007*	0.064±0.009
Volume density of granular layer (mm^0)	0.303±0.045	0.282±0.038	0.295±0.034
Volume density of capillary sinusoids (mm^0)	0.115±0.017	0.158±0.023	0.132±0.019
Number of neurons in stratum moleculare	92815.4±9445.1	87756.2±8290.1	88409.3±8500.5
Numerical density of neurons in stratum moleculare (mm^{-3})	5965.3±445.9	5331.6±412.8	5506.1±462.9

Table 3. continued

Parameters	Control group (n=15)	Exposured group (n=15)	Regenerated group (n=15)
Surface area of neurons in stratum moleculare (μm^2)	99.7± 7.2	95.5±8.5	99.4±7.7
Surface area of neurons´ nuclei in stratum moleculare (μm^2)	35.8±6.5	32.1±6.2	34.9±6.6
NCR of neurons in stratum moleculare	0.354±0.035	0.332±0.038	0.341±0.035
Mitotic index of neurons stratum moleculare	0.426±0.052	0.397±0.057	0.405±0.055
Apoptotic index of neurons in stratum moleculare	0.012±0.008	0.166±0.025*	0.072±0.013
Number of neurons in stratum gangliosum	555.5±34.2	401.9±32.8*	421.6±35.7
Numerical density of neurons in stratum gangliosum (mm^{-3})	65.4±4.5	51.2±4.8*	55.7±4.4
Surface area of neurons in stratum gangliosum (μm^2)	533.4±19.8	282.7±13.5*	324.3±15.3
Surface area of neurons´ nuclei in stratum gangliosum (μm^2)	286.6±13.5	114.3±11.2*	165.8±16.7
NCR of neurons in stratum gangliosum	0.354±0.038	0.388±0.039	0.352±0.035
Apoptotic index of neurons in stratum gangliosum	0.00±0.00	0.096±0.022*	0.048±0.007
Number of neurons in stratum granulosum	237193.4±15324.7	190093.2±13997.4	216013.5±15002.6
Numerical density of neurons in stratum granulosum (mm^{-3})	25769.3±2546.9	20022.5±2477.2	21799.4±2509.2
Surface area of neurons in stratum granulosum (μm^2)	84.9±4.3	83.2±4.9	84.1±5.1
Surface area of neurons´ nuclei in stratum granulosum (μm^2)	29.1±2.9	26.6±3.3	27.5±3.4
NCR of neurons in stratum granulosum	0.345±0.027	0.321±0.029	0.324±0.027
Mitotic index of neurons in stratum granulosum	0.417±0.045	0.387±0.041	0.409±0.044
Apoptotic index of neurons in stratum granulosum	0.011±0.006	0.143±0.021*	0.095±0.024
Number of capillary endothelial cells	114589.1±22802.1	159756.4±25112.9	147323.2±24347.7
Numerical density of capillary endothelial cells (μm^2)	30125.5±2371.6	41076.2±2795.1	39663.7±2660.9
Surface area of capillary endothelial cells (μm^2)	95.2±9.4	101.6±9.9	100.3±9.8

Micrographs of cerebellum tissue sections of experimental rats from all three groups show changes in its architecture. Mean values of the stereological analysis parameters of rat cerebellum were changed by comparing exposure in relation to the control group, as well as regenerated in relation to the exposure group. However, the mean values of these parameters of the cerebellum of rats from the regenerated group did not reach the values from the control group after six months of stay of rats in an environment without HFEMF. Volume density of stratum molecules, stratum gangliosum with Purkinje cells and stratum granulosum were decrease by 7-28% in the cerebellum of all rats exposure group (Fig. 1).

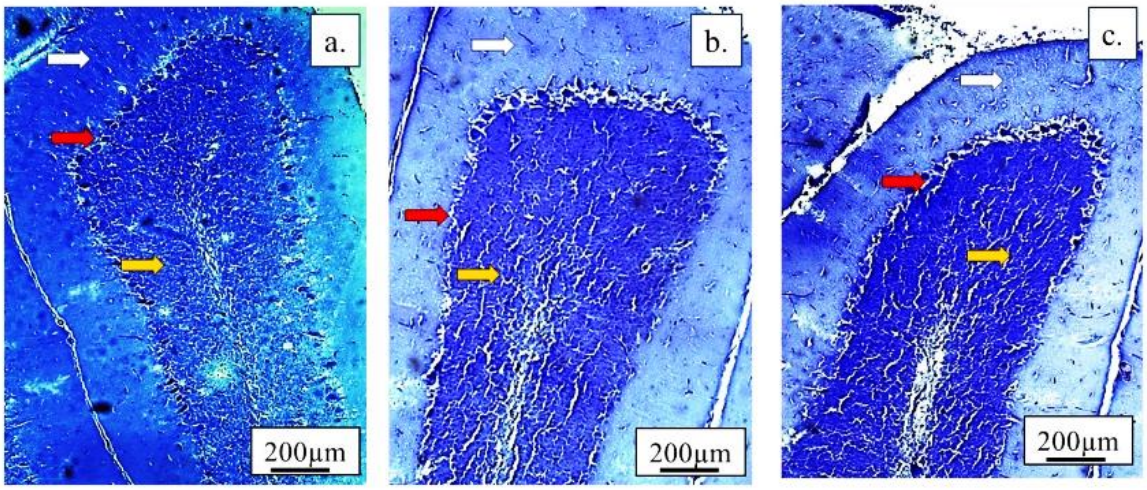

Figure 1. Micrographs of the histological cross-section of the rats´ cerebellum, Crazy-violet stain, magnification 40X. Changes in structure of cerebellum´s layers. Stratum moleculare (white arrows), stratum gangliosum (red arrows) and stratum granulosum (yellow arrows).
Control (a), exposured (b) and regenerated (c) rats.

Decrease in stratum gangliosum volume density with Purkinje cells in cerebellum was statistically significant ($p=0.0253$) in exposed rats. Volume density of stratum moleculare (Fig. 2), stratum granulosum (Fig. 3) and stratum gangliosum with Purkinje cells (Fig. 4 and 5) increased by 5-21% in the cerebellum of all rats regenerated group. After six months in the regenerated group, dendritic and pericaryal compartments regenerate and reconnect to the stratum granules (Fig. 4c red square brackets) and expand. Expansion of stratums moleculare, granulosum and gangliosum with Purkinje cells cause regeneration and reconnection of existing neurons and not an increase in their number in the regenerated group of rats. In these stratums are also a reorganization and reconnection of dendritic and pericaryal compartments of neurons in the regenerated group. Exposure of HFEMF rats leads to a change in the shape of neurons in their layers of the cerebellum cortex compared to neurons from the control group. The change in the shape of the neurons is not reversible and the neurons remain altered in the regenerated group. Increased apoptosis of all types of cerebellar neurons in rats from the exposure group is a consequence of confirmed disconnections between them. Changes in the values of stereological parameters of Purkinje cells are reversible because in a certain percentage they return to those from the control to the regenerated group. In the exposure group, there was a decrease in the number and change in the shape of Purkinje cells in the cerebellum of rats compared to the control group. In the regenerated group, there was no complete return of the number or correct shape of Purkinje cells in relation to the exposed. Microcaveolaes occur in the stratum gangliosum cerebellum exposure group of rats. In addition to reconnection, there is a decrease in microcaveolaes in the regenerated group. Reconnection between neurons in the cerebellum regenerated group was demonstrated by reassembling SNXS25 proteins in their cytoplasm (Fig. 5). All stereological parameters of rat cerebellar blood vessels from the exposed and regenerated groups of our study showed higher values compared to the control group. In the regenerated group, the changed architecture of blood vessels from the exposure group remains.

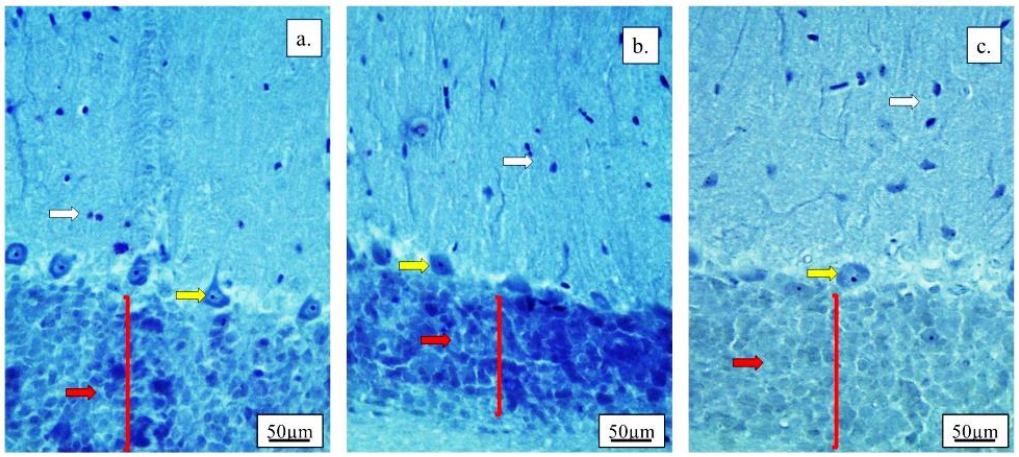

Figure 2. Micrographs of the histological cross-section of the rats´ cerebellum, Crazy-violet stain, magnification 100X. Changes in structure of cerebellum´s layers. Stratum moleculare (white arrows), Purkinje cells (yellow arrows) and stratum granulosum (red arrows); red square brackets show the different thickness of stratum granulosum. Control (a), exposured (b) and regenerated (c) rats.

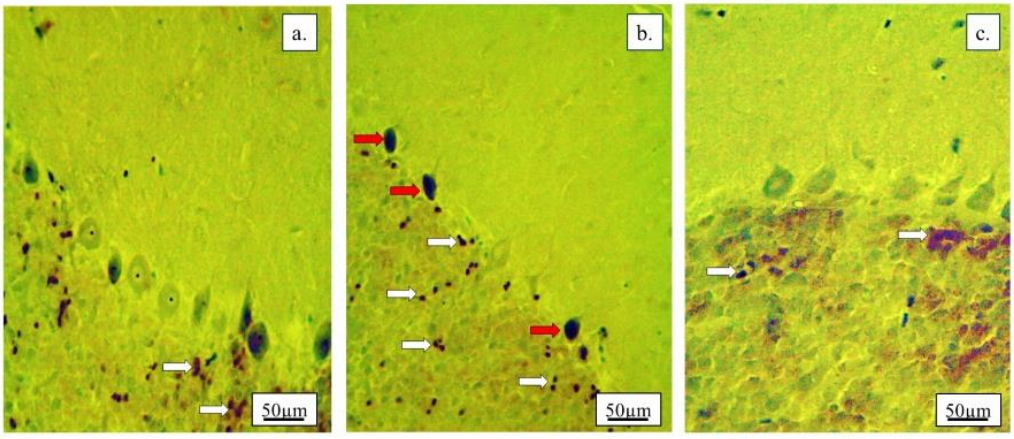

Figure 3. Micrographs of the histological cross-section of the rats´ cerebellum cortex, immunohistochemical detection caspase-3, magnification 100X. Detection apoptotic neurons. Apoptotic neurons in stratum granulosum (white arrows) and apoptotic Purkinje cells (red arrows). Control (a), exposured (b) and regenerated (c) rats.

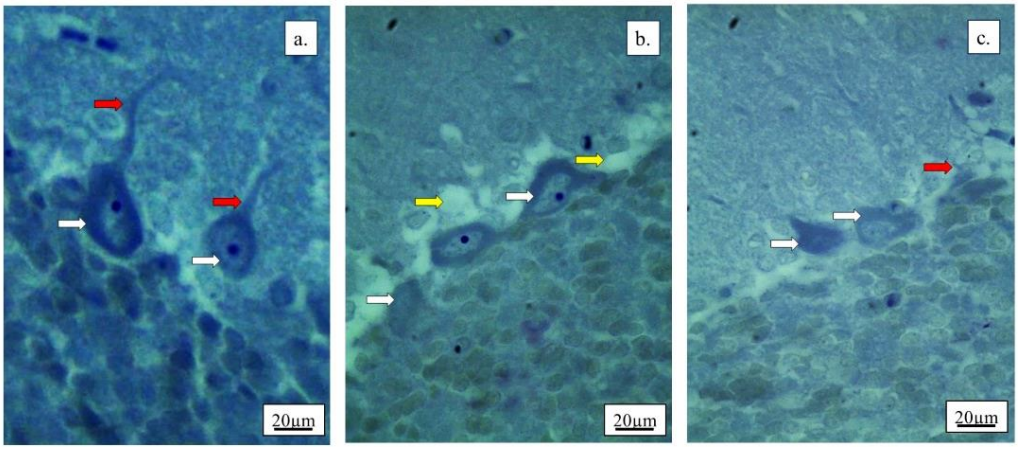

Figure 4. Micrographs of the histological cross-section of the rats´ cerebellum cortex, Crazy-violet stain, magnification 250X. Detection microcaveolaes and dendrites of Purkinje cells in stratum gangliosum. Dendritic compartment of Purkinje cells (red arrows), pericaryal compartment of Purkinje cells (white arrows), microcaveolaes (yellow arrows).
Control (a), exposured (b) and regenerated (c) rats.

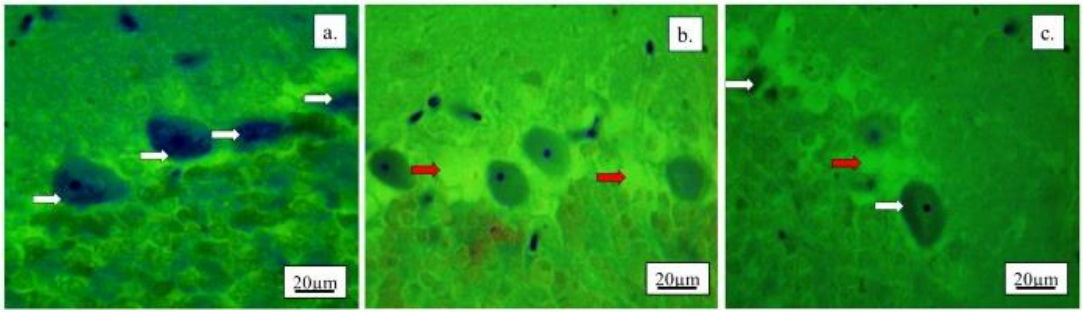

Figure 5. Micrographs of the histological cross-section of the rats´ cerebellum cortex, Immunohistochemical detection SNX25 protein, magnification 250X. Reconnection of neurons in stratum gangliosum. Detection SNX25 protein in Purkinje cells (white arrows), microcaveolaes (red arrows) in stratum gangliosum. Control (a), exposured (b) and regenerated (c) rats.

Histological and stereological analysis of cerebral tissues

All mean values of the parameters of the stereological analysis of the rat cerebrum were changed with comparing exposure in relation to the control group, as well as regenerated in relation to the exposure group (Tab. 4).

Table 4. Stereological parameters of cerebral cortex and basal ganglia tissues in control and both experimental groups of rats, value are shown as mean ± SD (*p<0.05; t-test).

Parameters	Control group	Exposured group	Regenerated group
Volume density of molecular neurons (mm^0)	0.114±0.011	0.100±0.009	0.104±0.009
Volume density of granular neurons (mm^0)	0.152±0.012	0.141±0.013	0.143±0.012
Volume density of pyramidal neurons (mm^0)	0.124±0.010	0.111±0.009	0.112±0.010
Volume density of basal ganglia neurons (mm^0)	0.105±0.008	0.095±0.007	0.099±0.008
Volume density of nerve fibers in basale ganglion (mm^0)	0.164±0.025	0.147±0.021	0.159±0.025
Volume density of capillary sinusoids (mm^0)	0.134±0.018	0.177±0.028	0.169±0.026
Number of molecular neurons	126375.6±15067.2	110373.4±14888.3	120150.1±14362.1
Numerical density of molecular neurons (mm^{-3})	11778.4±1158.2	10066.5±1014.7	10975.3±1053.5
Surface area of molecular neurons (μm^2)	82.3±2.1	77.5±1.8	81.6±22
Surface area of molecular neurons´ nuclei (μm^2)	42.3±1.9	40.5±1.7	44.8±1.9
NCR of molecular neurons	0.514±0.044	0.529±0.046	0.549±0.049
Mitotic index of molecular neurons	0.998±0.087	1.105±0.108	1.148±0.117
Apoptotic index of molecular neurons	0.027±0.016	0.091±0.058*	0.034±0.068
Number of granular neurons	162713.5±11756.3	131673.9±10321.8	149024.7±11476.0
Numerical density of granular neurons (mm^{-3})	15629.5±1432.7	13997.4±1385.3	14272.2±1566.9
Surface area of granular neurons (μm^2)	222.4±7.9	199.8 ±7.7	214.3±7.4
Surface area of granular neurons´ nuclei (μm^2)	149.1±4.2	130.4±4.3	142.9±4.1

Table 4. continued

Parameters	Control group	Exposured group	Regenerated group
NCR of granular neurons	0.674±0.075	0.653±0.069	0.667±0.067
Mitotic index of granular neurons	0.292±0.031	0.207±0.027	0.209±0.029
Apoptotic index of granular neurons	0.009±0.002	0.039±0.011*	0.016±0.008
Number of pyramidal neurons	133242.2±10113.5	110145.6±10076.4	118795.3±10904.6
Numerical density of pyramidal neurons (mm^{-3})	12848.9±1112.8	11427.7±1089.2	12053.5±1155.6
Surface area of pyramidal neurons (μm^2)	284.3±8.8	265.4±8.4	292.3±8.9
Surface area of pyramidal neurons´ nuclei (μm^2)	76.6±2.2	71.3±2.4	73.1±2.5
NCR of pyramidal neurons	0.257±0.027	0.244±0.029	0.261±0.025
Apoptotic index of pyramidal neurons	0.005±0.001	0.032±0.009*	0.014±0.0004
Number of basal ganglia neurons	87669.4±5796.4	79483.3±5955.3	84094.6±5509.3
Numerical density of basal ganglia neurons (mm^{-3})	7932.4±256.4	7689.7±279.6	7814.6±299.5
Surface area of basal ganglia neurons (μm^2)	105.6±4.6	78.4±3.8	89.2±3.5
Surface area of basal ganglia neurons´ nuclei (μm^2)	31.9±2.9	27.6±2.1	29.1±2.2
NCR of basal ganglia neurons	0.289±0.022	0.331±0.026	0.315±0.025
Apoptotic index of basal ganglia neurons	0.00±0.00	0.104±0.011*	0.055±0.008
Number of capillary endothelial cells	129405.7±18424.5	153376.9±19842.2	144092.4±18788.1
Numerical density of capillary endothelial cells (μm^2)	35210.6±2603.4	45225.6±3196.2	41473.3±2833.3
Surface area of capillary endothelial cells (μm^2)	97.1±8.8	108.2±8.9	105.5±8.9

Also, the mean values of these parameters of the cerebrum of rats from the regenerated group did not reach the values from the control group after six months of stay of rats in an environment without HFEMF. Mean volume densities of stratum moleculare, stratum granulosum, stratum pyramidal, basal ganglia, and nerve fibre in the basal ganglion decreased by 7-12% in the cerebrum of all rats exposure group. Mean values of the same parameters increased by 1-8% in the cerebrum of all rats regenerated group compared to the cerebrum of rats exposure group (Fig. 6). The volume density of capillary sinusoids had the highest value in the exposure group, while in the regenerated group it remained elevated. This is an example that HFEMF affects the volume expansion of capillary sinusoids (Fig. 7). In the regenerated group there was an increase in the same stereological parameters of the stratum molecular in cerebral cortex in rats compared to the exposed, except for the apoptotic index neurons which decreased. In the stratum moleculare regenerated group, dendritic and pericaryal compartments of neurons reorganize and reconnect after the action of HFEMF. However, the change in the number and shape of neurons is not reversible.

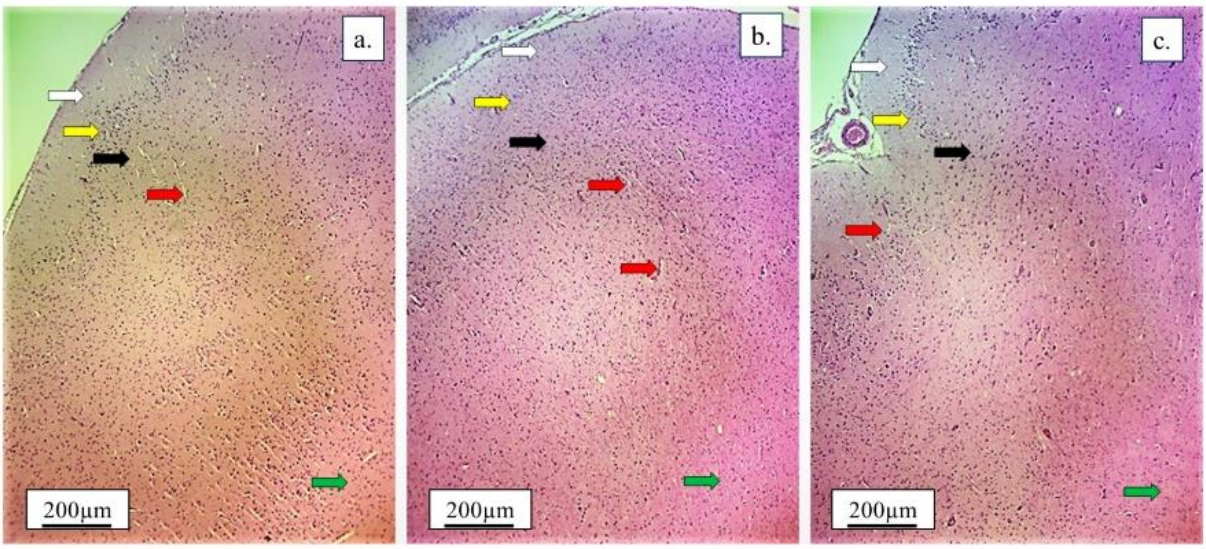

Figure 6. Micrographs of the histological cross-section of the rats´ cerebral cortex, Mallory Azan trichrome stain, magnification 10X. Changes in structure of cerebrum´s layers. Stratum moleculare (white arrows), stratum granulosum (yellow arrows), stratum pyramidal (black arrows), basal ganglia (green arrows) and capillary sinusoids (red arrows).
Control (a), exposured (b) and regenerated (c) rats.

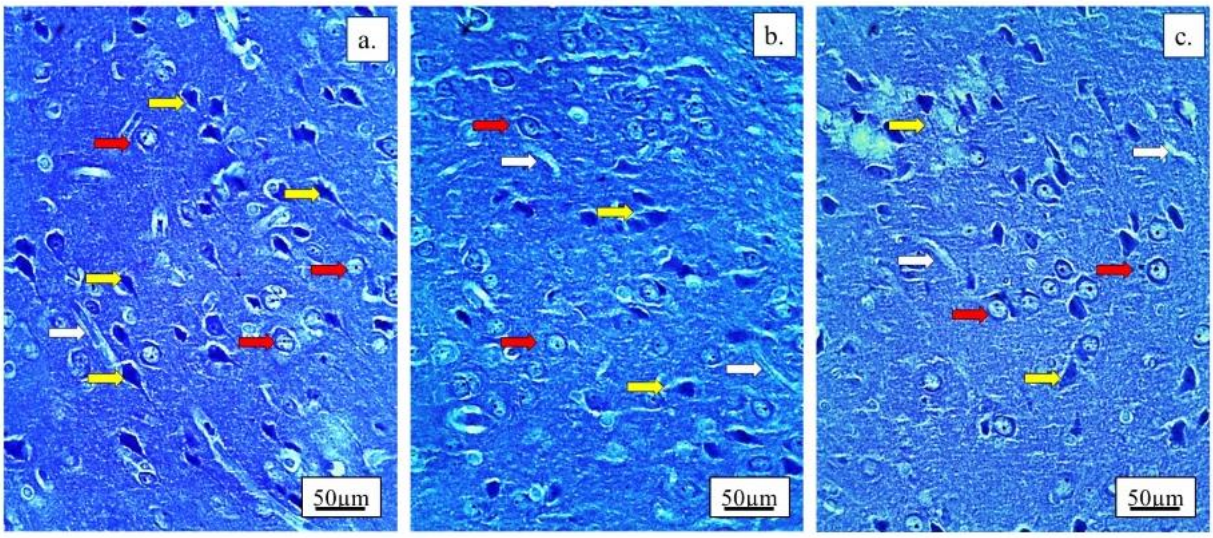

Figure 7. Micrographs of the histological cross-section of the rats´ cerebral cortex, Crazy-violet stain, magnification 100X. Changes in shape of neurons in stratum moleculare. Moleculare neurons (red arrows), granular neurons (yellow arrows) and capillary sinusoids (white arrows).
Control (a), exposured (b) and regenerated (c) rats.

A statistically significant increase in the apoptotic index in the exposure group was detected by immunohistochemical detection of caspase-3 in sections of cerebral cortex in rats (Fig. 8). Microcaveolaes and apoptotic neurons disappeared in the regenerated group because neuronal regeneration was aided with increased blood flow, due to an increase in the volume of the capillary sinusoids of the molecular layer of the cerebral cortex (Fig. 9). The increase in the value of the volume density of the stratum granulosum in the cerebral cortex in the rats in the regenerated group is a consequence of the regeneration and reconnection of neurons, and not an increase in their number.

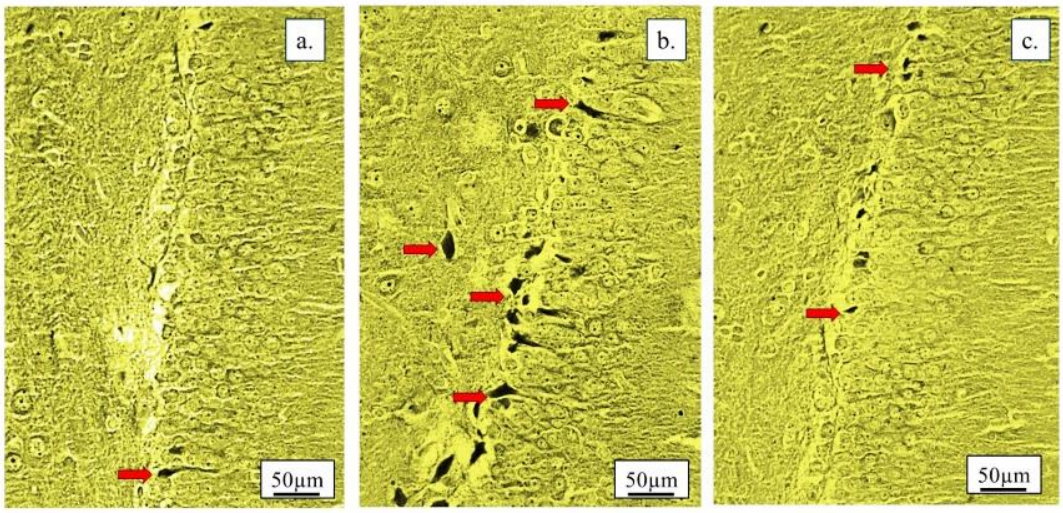

Figure 8. Micrographs of the histological cross-section of the rats´ cerebral cortex, immunohistochemical detection caspase-3, magnification 100X. Detection apoptotic neurons. Molecular and granular neurons in apoptosis (red arrows).
Control (a), exposured (b) and regenerated (c) rats.

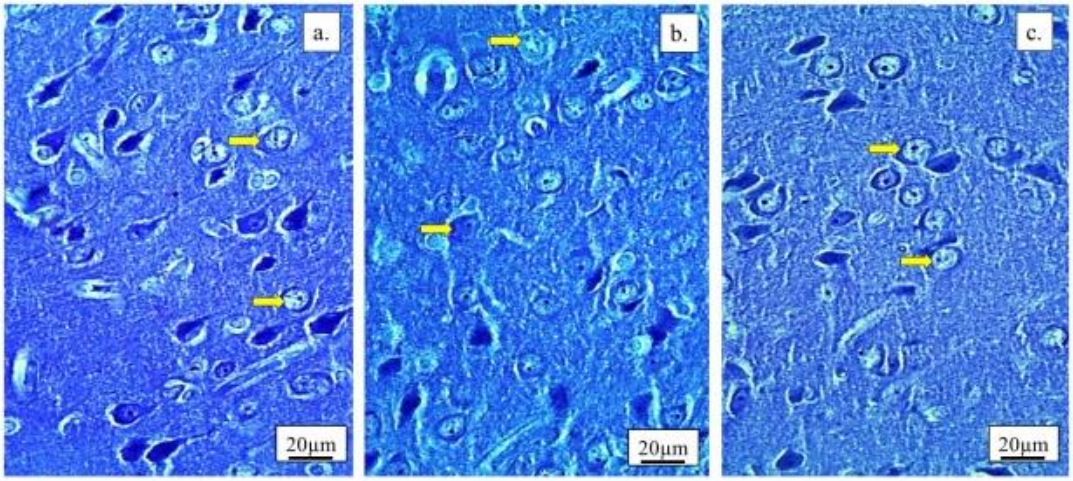

Figure 9. Micrographs of the histological cross-section of the rats´ cerebral cortex, Crazy-violet stain, magnification 150X. Changes in shape of neurons in stratum granulosum. Granular neurons (yellow arrows). Control (a), exposured (b) and regenerated (c) rats.

Neurons in apoptosis were very small in size, blood vessels were dilated, and there was no microcaveolaes in the stratum of the granular cerebral cortex in the exposure group compared to the control. Apoptotic neurons and microcaveolaes disappeared in regenerated groups (Fig. 10) because there were regeneration of neuron components and increased blood flow to the granular stratum.

Generally, in the granular layer of the cerebral cortex in the regenerated group of rats, there is a change in the arrangement of neurons due to their reconnection and regeneration. In the regenerated group, all stereological parameters of the stratum pyramidal in cerebral cortex increased in relation to the exposed. Also, in this group, dendritic and pericaryal compartments regenerate and reconnect to the stratum pyramidal and expand and establish proper arrangement (Fig. 11 and 12). Proper arrangement of the pyramidal layer in regenerated group of rats causes regeneration and reconnection of pyramidal neurons and not an increase in their number.

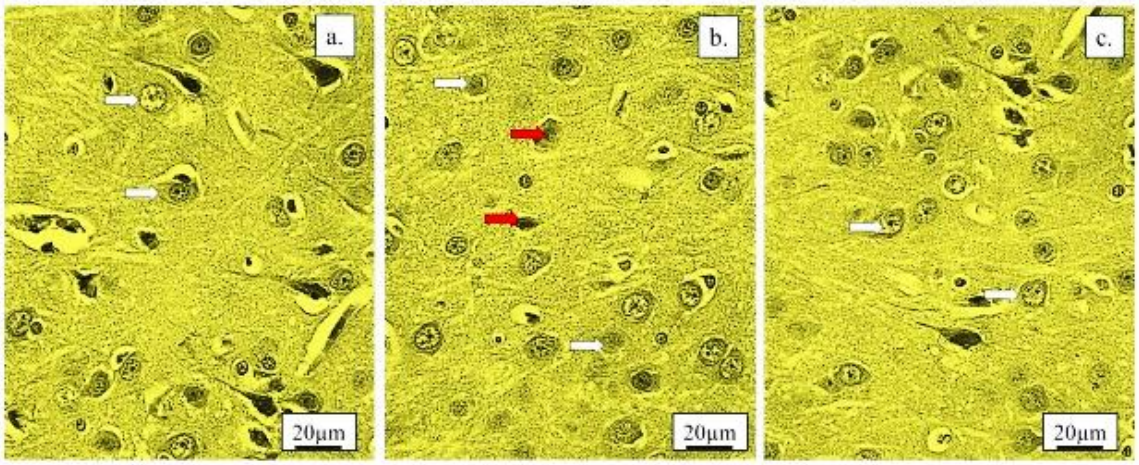

Figure 10. Micrographs of the histological cross-section of the rats´ cerebral cortex, immunohistochemical detection caspase-3, magnification 150X. Detection apoptotic neurons. Granular neurons (white arrows), granular neurons in apoptosis (red arrows). Control (a), exposured (b) and regenerated (c) rats.

The number of pyramidal cells in the regenerated group of rats increased slightly compared to the exposure group but did not return to the value it had in the control group. A statistically significant increase in the apoptotic pyramidal stratum index in the exposed group of rats compared to the control and regenerated groups (Fig. 13) were detected by immunohistochemical detection with caspase-3. Also, in the exposed group the blood vessels were dilated and there was the presence of microcaveolaes in the stratum pyramidal in the cerebral cortex. In the regenerated group on the one hand there was no presence of apoptotic neurons, while on the other hand there was the presence of regeneration dendritic compartment of pyramidal neurons. There was an increase in the length of the neurite's outlet, the blood supply to the pyramidal stratum, and the disappearance of the microcaveolaes.

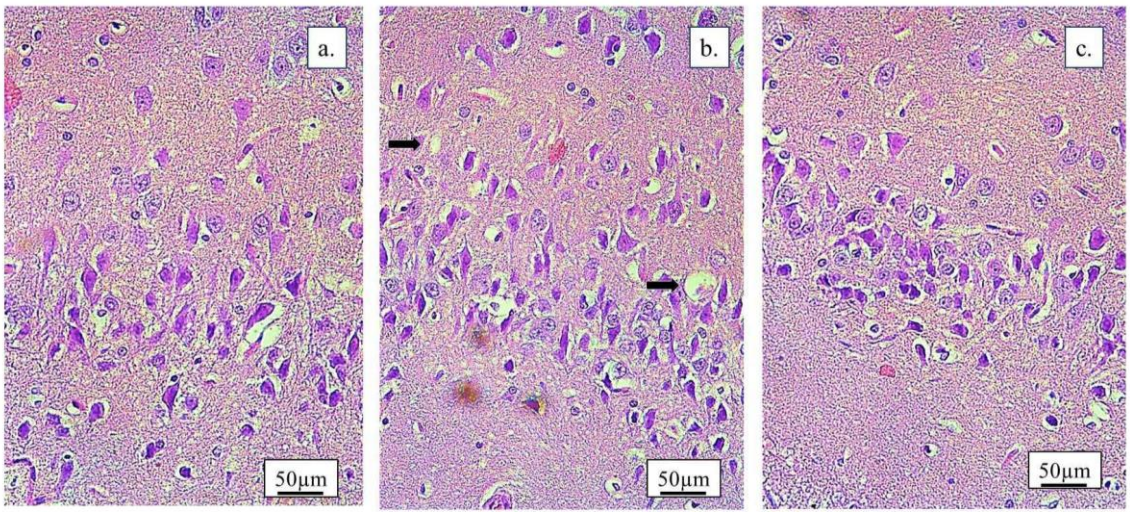

Figure 11. Micrographs of the histological cross-section of the rats´ cerebral cortex, Crazy-violet stain, magnification 100X. Stratum pyramidal, changes in shapes of pyramidal neurons and microcaveolaes (black arrows). Control (a), exposured (b) and regenerated (c) rats.

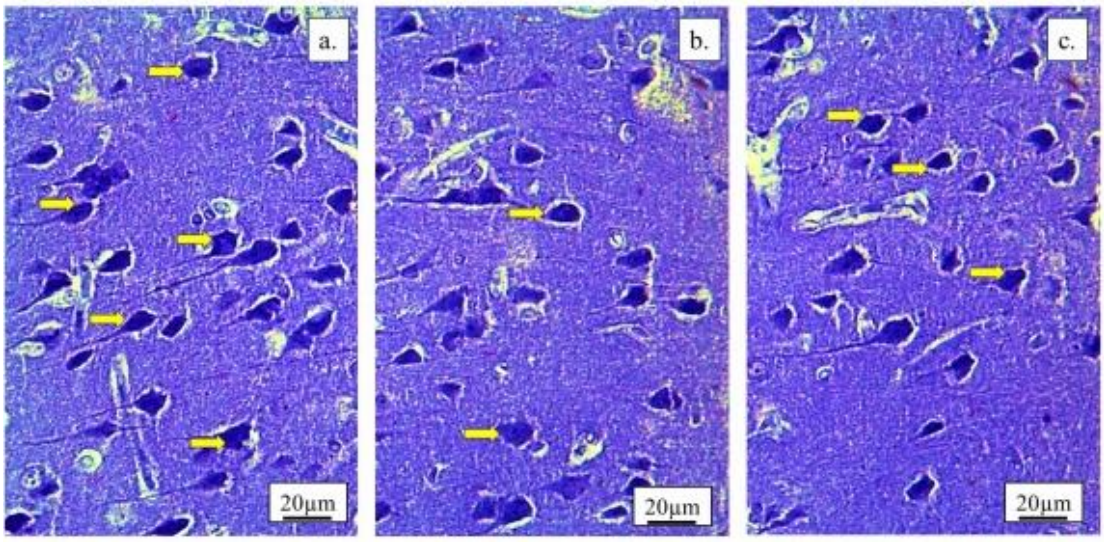

Figure 12. Micrographs of the histological cross-section of the rats´ cerebral cortex, Crazy-violet stain, magnification 150X. Changes in shape of neurons in stratum pyramidal. Pyramidal neurons (yellow arrows). Control (a), exposured (b) and regenerated (c) rats.

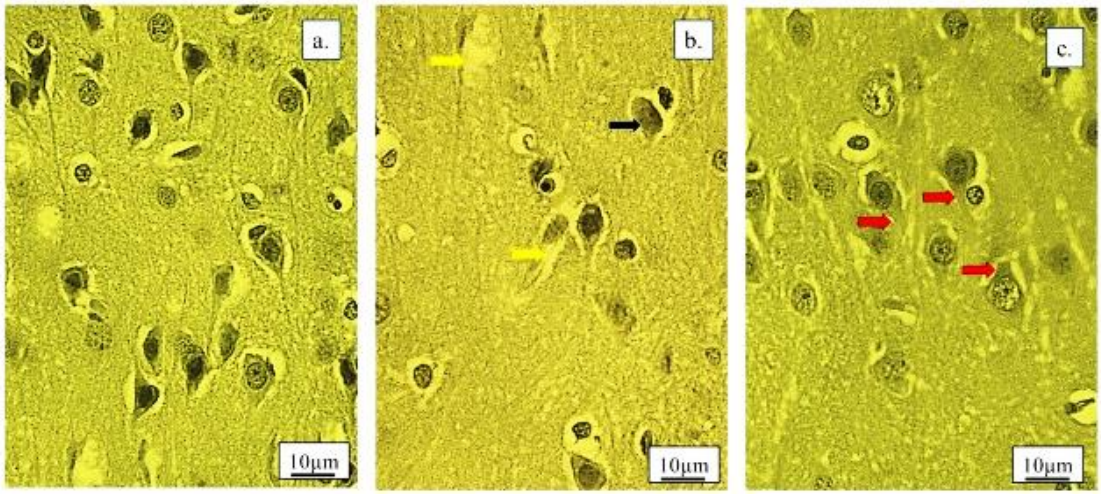

Figure 13. Micrographs of the histological cross-section of the rats´ cerebral cortex, immunohistochemical detection caspase-3, magnification 200X. Detection apoptotic neurons. Pyramidal neurons in apoptosis (black arrows), microcaveolaes (yellow arrows) and regeneration dendritic compartment of pyramidal neurons. Control (a), exposured (b) and regenerated (c) rats.

Generally, the stratum pyramidal of the cerebral cortex changes in the appearance, connection, and arrangement of pyramidal neurons due to their reconnection and regeneration into a regenerated group of rats. In the regenerated group there was an increase in the same stereological parameters of the basal ganglia in cerebrum in rats compared to the exposed one, except for the apoptotic index neurons which decreased. Regeneration and reconnection of basal ganglion neurons was intensive in the regenerated group of rats (Fig. 14). After regeneration, the neurons of the basal ganglia do not return to the shape they had at the beginning of the experiment, but the volume of dendrite components increases. The SNXS25 protein detects the cytoskeletal components of basal ganglion neurons that are crucial in their regeneration after a six-month reconnection (Fig. 15). Degree of regeneration of all types of analysed neurons of cerebellum and cerebrum of rats in percent directly shows which of them has the best ability to reconnect and regenerate after six months of keeping exposed rats in the environment without HFEMF. Neurons with a larger dendritic network volume, such as

Purkinje cells, pyramidal neurons, and basal ganglion neurons, had a higher percentage of regeneration after reconnection. Note that none of the types of cerebellar and cerebellar neurons returned to the size of the surface area to the value of cerebellar and cerebellar neurons in the control group of rats.

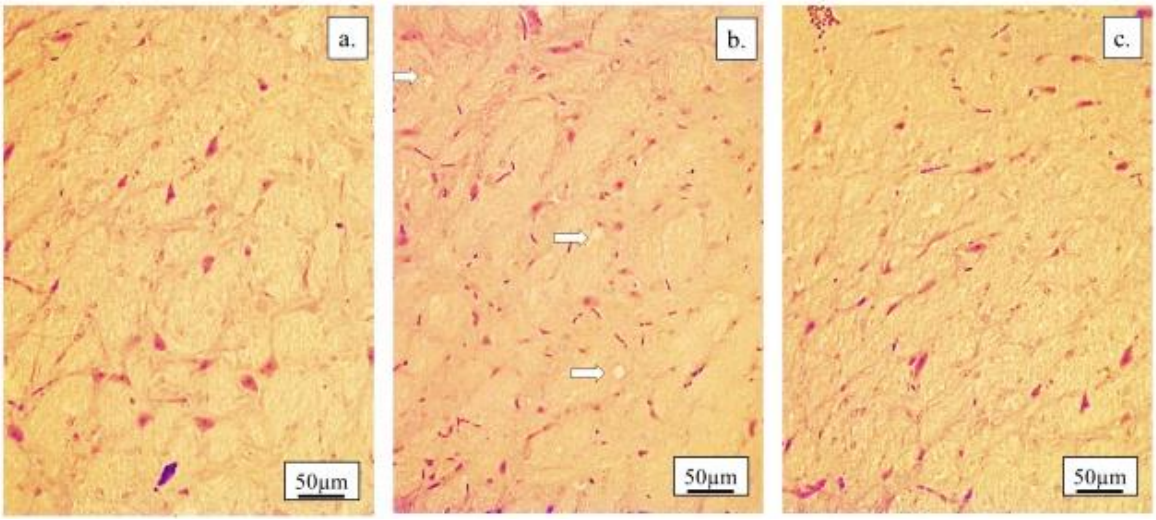

Figure 14. Micrographs of the histological cross-section of the rats´ basal ganglia, Haematoxylin-Eosin stain, magnification 100X. Regeneration dendritic compartments of basal ganglia neurons and microcaveolaes (white arrows). Control (a), exposured (b) and regenerated (c) rats.

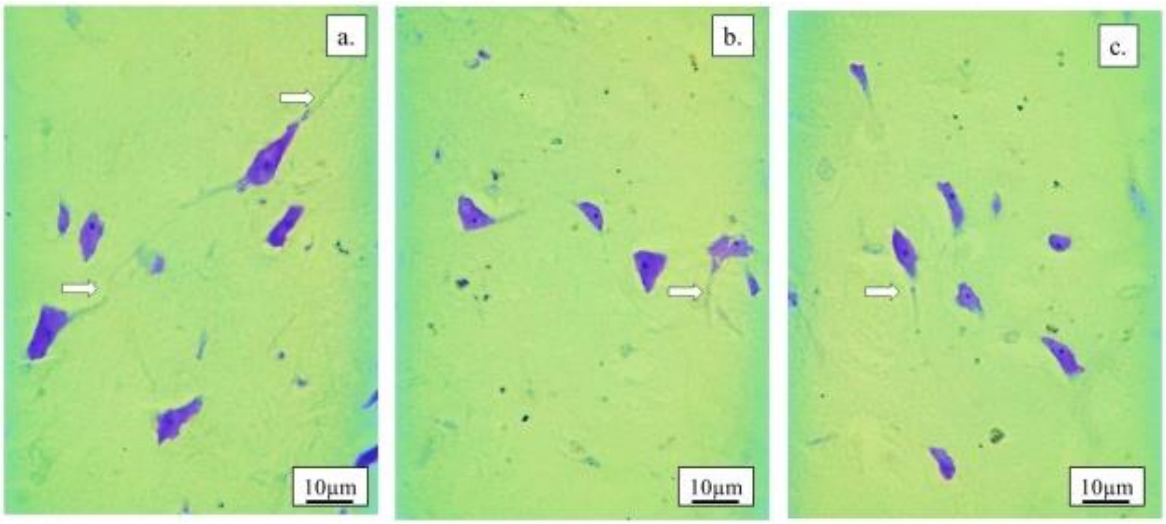

Figure 15. Micrographs of the histological cross-section of the rats´ basal ganglia, immunohistochemical detection SNX25 protein, magnification 250X. Regeneration dendritic compartments of basal ganglia neurons (white arrows). Control (a), exposured (b) and regenerated (c) rats.

Ultrastructural analysis of cerebellar neurons

Changes in the nuclei and membranes of neurons from the stratum gangliosum cerebellum of rats after the influence of HFEMF and after the period of their regeneration were ultrastructural analysed and presented on TEM electron micrographs. HFEMF reduces the

volume of the nucleus (Fig.16b), initiates the process of apoptosis (Fig. 16c), causes a decrease in the proportion of euchromatin relative to heterochromatin (Fig. 16d) and initiates the process of nucleus fragmentation (Fig.16e) in gangliosum neurons´ in exposure cerebellum relative to control group (Fig. 16a). The nuclei in the gangliosum neurons of the cerebellum in the regenerated group of rats is return to their normal shape and volume, and in their heterochromatin are numerous centres of transcriptional activity and the transition from heterochromatin to euchromatin (Fig. 16f). HFEMFs cause plasma membrane separation, neuronal disconnection, and the appearance of endocytotic vesicles (Fig. 17b). Microcaveolaes are found in the disconnected space (Fig. 17c). The space between two disconnected neurons is several times wider than normal neurons (Fig. 17e) in the gangliosum neurons´ in exposure cerebellum relative to the control group (Fig. 17a). Plasma membranes in the gangliosum neurons in the cerebellum in the regenerated group of rats is reduced the space between them many times over, return to their normal shape and reconnect with each other (Fig. 17f). Reconnection of gangliosum neurons enables their regeneration and restoration of function.

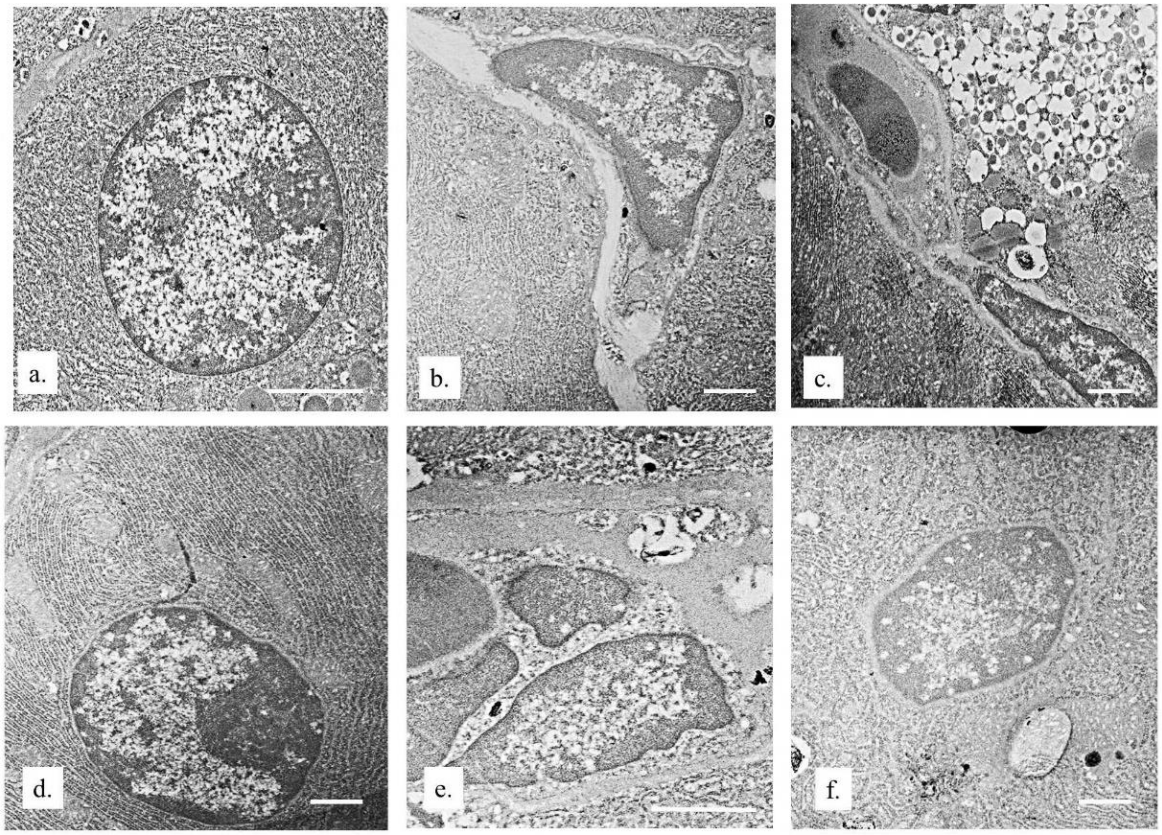

Figure 16. Transmission electron micrographs of the cerebellum neurons from stratum gangliosum. Thin section. Ck18.10/02/2021/11:15:25. TEM Mode Imagining. HV=80.0kV. Direct Mag:26000x/ATM Camera System. Changes in surface area of gangliosum neurons´ nuclei. Control (a), exposured (b, c, d, e) and regenerated (f) rats.

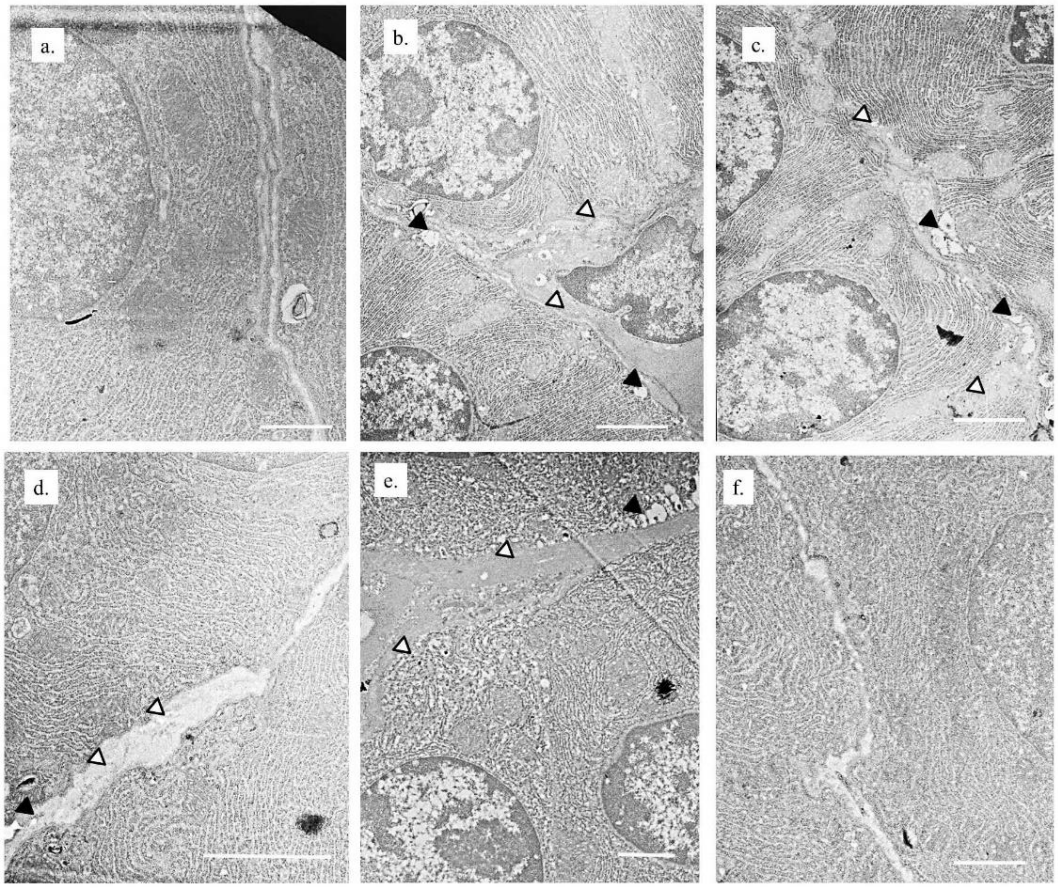

Figure 17. Transmission electron micrographs of the cerebellum neurons from stratum gangliosum. Thin section. Ck18.10/02/2021/11:45:05. TEM Mode Imagining. HV=80.0kV. Direct Mag:18000x/ATM Camera System. Changes in plasma membrane of gangliosum neurons: microcaveolaes (black arrows) and the space between plasma membranes of two disconnected neurons (white arrows). Control (a), exposured (b, c, d, e) and regenerated (f) rats.

Ultrastructural analysis of cerebral neurons

Changes in the nuclei and membranes of neurons from the stratum gangliosum cerebrum of rats after the influence of HFEMF and after the period of their regeneration were ultrastructural analysed and presented on transmission electron microscope (TEM) electron micrographs. HFEMF reduces nuclear volume (Fig. 18b), homogenizes nuclear chromatin (Fig. 18c), causes a decrease in euchromatin relative to heterochromatin, initiates apoptosis (Fig.18d) and initiates nuclear fragmentation (Fig. 18e) in pyramidal neurons´ in exposure cerebrum in relative to the control group (Fig. 18a). Nuclei in pyramidal neurons in cerebrum return to their normal shape and volume in the regenerated group of rats, and their heterochromatin contains numerous centres of transcriptional activity and the transition from heterochromatin to euchromatin (Fig. 19f). HFEMFs cause separation of plasma membranes, disconnection of two neurons and the appearance of microcaveolaes in the disconnected space (Fig. 19b), the space between two disconnected neurons is several times wider than normal filled with most likely intercellular substances (Fig. 19c), plasma membranes of two disconnected neurons contain numerous endocrine and reverts according to the cytoplasm (Fig. 19e) in the pyramidal neurons´ in exposure cerebrum relative to the control group (Fig. 19a). Plasma membranes in pyramidal neurons in the cerebrum in the regenerated group of rats are reduced the space between them many times over, return to their normal shape and reconnect with each other (Fig. 19f). Reconnection of pyramidal neurons enables their regeneration and restoration of function.

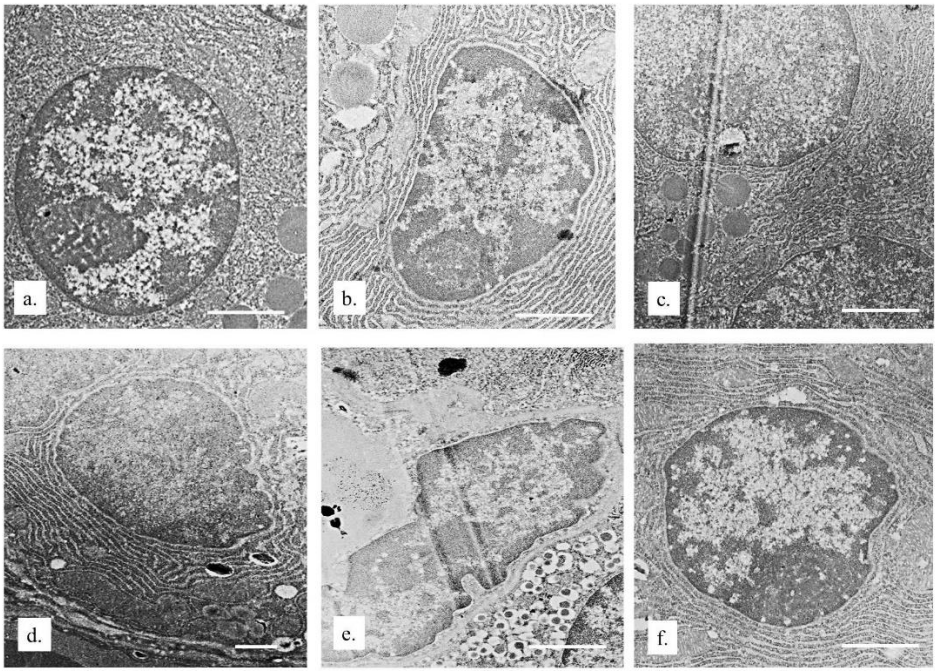

Figure 18. Transmission electron micrographs of the cerebrum neurons from stratum gangliosum. Thin section. Ck18.10/02/2021/11:30:20. TEM Mode Imaginig. HV=80.0kV. Direct Mag:24000x/ATM Camera System. Changes in surface area of pyramidal neurons´ nuclei.
Control (a), exposured (b, c, d, e) and regenerated (f) rats.

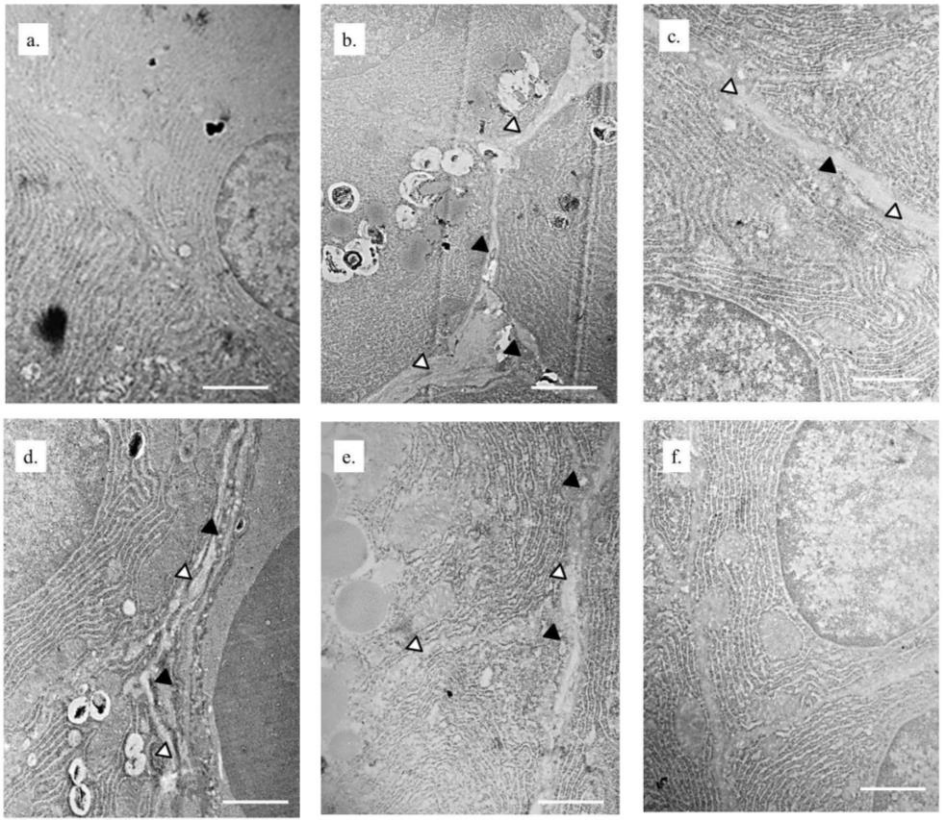

Figure 19. Transmission electron micrographs of the cerebrum neurons from stratum gangliosum. Thin section. Ck18.10/02/2021/10:25:35. TEM Mode Imagining. HV=80.0kV. Direct Mag:26000x/ATM Camera System. Changes in surface area of pyramidal neurons´ plasma membrane: microcaveolaes (black arrows) and the space between plasma membranes of two disconnected neurons (white arrows).
Control (a), exposured (b, c, d, e) and regenerated (f) rats.

DISCUSSION

Our study showed the potential of HFEMF in treatment of neurodegenerative diseases. This study shows the yet unseen findings that HFEMF can induce the regeneration of cerebellar and cerebral tissues of rats after their exposure to said fields. Values of all haematological parameters in the regenerated group returned to their initial ones, very similar to the control group. Changes in values of RBC in rats exposed to HFEMF such as regenerated group are consequence of increased capacity for oxygen by cells (ALGHAMDI *et al.,* 2012; SHOJAEIFARD *et al.,* 2018; GHADHBAN and MHEIBES, 2018). RBC volume and size distribution are parameters that did not change in the study, which means that HFEMF don´t disrupt qualitative and functional haematopoiesis (WYSZKOWSKA *et al.,* 2018; ZHANG *et al.,* 2020). HFEMF may cause an increase (SANI *et al.,* 2018; ADEBAYO *et al.,* 2019), as in study, or a decrease (ROSADO *et al*., 2018) in WBC and LYM levels in rat blood. Consequences of HFEMF activity are changes in surface receptors in cell membranes of immune system cells and antibody production stimulation (SURCEL *et al.,* 2017) as well as increased fibrinogen in blood plasma (HOSSEINABADI *et al.,* 2019; AKBARI *et al.,* 2020). In present work, increase of thrombocytopoiesis in rats terminates after animals leave HFEMF, thus increasing the platelet number to initial values. An increase in the value of PLV and an unchanged value of RCD in exposed rats is a finding unique to this paper. A shorter interval of HFEMF rat exposure leads to more unstable and reversible, while a longer interval leads to more stable and long-lasting changes in blood composition and dynamism compared to a later period when field´ influence is excluded (DELWATTA *et al.,* 2018; RECORDATI *et al.,* 2019). In regenerated group of rats, values of altered biochemical parameters of blood have returned to initial values. Consequence of the increase of triglycerides is due to intensified lipid peroxidation in cells (KIPRIYANOV *et al.,* 2015) and increased repair of cell membranes after the treatment of HFEMF (BELLOSSI *et al.,* 1998). Also, the glucose concentration was in normal values during the period of regeneration (PARAŠ *et al.,* 2017). Reason for changed value of creatinin in serum of rats due to action of EMF is explained with fact that EMF stimulates the work of immune system, which burdens work of kidneys (BORZOUEISILEH *et al.,* 2020). In regenerated group values of liver enzymes in blood of rats returned to very similar to control group in our study. Our results of a reversible change in concentration of liver enzymes in blood of rats are just another proof that liver tolerates HFEMF exposure very well (SANI *et al.,* 2018). In our work, increase in GPT and GGT values in blood of rats proves the increased metabolism of lipids and carbohydrates and protein catabolism in hepatocytes of rats from the exposure group (OLTEAN-DAN *et al.,* 2019). Reason for decrease in electrolyte concentration is explained by disruption of operation of ion pumps on cell membranes neurons by HFEMF (DOGAN *et al.,* 2017). In regenerated group, mean electrolyte didn´t return to initial values as in control group.

Although in the experimental part of study, all three groups of animals were not isolated from the existing (ambient) effects of electromagnetic fields, differences in brain morphology were observed. Neurons of the cerebellum and cerebrum are sensitive to the action of HFEMF, so that the fields act excitatory (REES *et al.,* 2017) and change the work of ion pumps on the plasma membranes of neurons (OL'SHEVSKAIA *et al.,* 2009; KANDEL *et al.,* 2017). HFEMF reduces the membrane potential of neurons, changes transmission of neurotransmitters and hyperpolarizes the postsynaptic membranes of neurons (TAN *et al.,* 2019; SHARMA *et al.,* 2021). From the histological point of view, HFEMF act on the cerebellum through the membranes of neurons, causing their reconnection and communication (ACOSTA *et al.,* 2018; WYSZKOWSKA *et al.,* 2019). In our work, reconnection of disconnected neurons in regenerated group cerebellums by increasing the expression of microtubule SNX25 protein and increasing dendritic and pericaryal compartments of Purkinje cells was registered. Reconnection of neurons after HFEMF exposure occurs by stimulating the transfer of action potential through them (PASHUT *et al.,* 2011). Stimulation of the work of a neuron is performed through

depolarization of its membranes, which leads to the initiation of the action potential (SCHNABEL and STRUIJK, 1999). Electric currents are a very important activator and catalyst in the regeneration of neurons because they generate ionic forces that react with the electrical activity of neurons (PETRIDOU *et al.,* 2009) and affect the elongation and growth of neurons (KIM *et al.,* 2008). Regeneration of rat cerebellum neurons from the regenerated group in our study was aided by an increase in blood vessel volume and increased vascularization of nerve tissue. Reconnection of individual neurons of the cerebellum was a prerequisite for the coupling effect of nerve tissue regeneration (KISHORE *et al.,* 2019). In our study, the altered architecture in all strata of the cerebral cortex and basal ganglia of rats from the exposure and regenerated group in relation to the control group was presented. Analysis of the cerebral cortex of the exposure group was difficult because the extended boundary areas of the layers contained multiple types of neurons characteristic of both layers. Regeneration of cerebral neurons led to the establishment of their reconnection and not to the return of their initial number. HFEMF did not cause histopathological changes in the cerebral tissues of exposure rats such as inflammation, cysts, necrosis, hydrocephalus, or thrombosis. Disconnection of neurons leads to disruption of information flow, influx of nutritional and stimulatory factors between neurons, remodelling of neurons, reduction of their NCR and increased apoptosis (IKONOMIDOU and KAINDL, 2011). The values of stereological parameters of all cortex layers, basal ganglia and nerve fibre in basal ganglia in the regenerated group of rat cerebrum have increased due to the reconnection between neurons. Reconnection and regeneration of neurons in the cerebral cortex layer and basal ganglia are consequences of dendritogenesis and increase in the volume of neurons´ pericaryal in them (WILSON and MONGIN, 2019). Neurorestoration and proper functioning of neurons is possible through the stimulation of neuroglia, astrocytes and the immune system with EMF (ISAKOVIĆ *et al.,* 2019).

Another condition for the reconnection and dendritogenesis of neurons is the establishment of a correct cytoskeleton in them (IACOMINO *et al.,* 2020). In our work, the regeneration of cytoskeleton was demonstrated through detection of SNX25 protein in cerebral neurons of rats from the regenerated group. Influence of EMF on proper arrangement of cytoskeletal proteins in damaged neurons is presented in the paper on neuroregeneration in people with Alzheimer's disease and in order to improve memory (AHMAD *et al.,* 2020). Neurorestoration occurs in all layers of the cortex due to reconnection, regeneration and nerve plasticity caused with HFEMF radiation (GEMINIANI *et al.,* 2018). Plasticity of cerebral cortex neurons of regenerated rat group is reflected in regeneration of dendritic and pericaryal compartments of neurons and not in the increase in mitotic index. In our work, the existence of potential nerve tissue regeneration is proven, in which the volume density of dendrites increases and not the number of neurons (PETRIDOU *et al.,* 2009; KIVRAK *et al.,* 2017). Endogenous electromagnetically stimulation of receptor proteins leads to the rehabilitation of pyramidal cells. The neurons of the basal ganglia in our study have intensively regenerated. They did not return to the shape they had at the beginning of the experiment, but their volume of pericaryon increased as well as volume of dendrite components (SALFORD *et al.,* 2003; PIVOVARENKO, 2019; BAI *et al.,* 2021). Main drivers of dendritic regeneration were signalling proteins on the membranes of neurons driven with EMF energy. Signal proteins further drive impulses to cytoskeletal proteins that are arranged in direction of the differentiated neurons (BAI *et al.,* 2021). EMF can improve memory in rats with Alzheimer's disease, regenerate ischaemic brain, stimulate neuroregeneration, induce neuronal differentiation with endogenous growth factors, and activate epidermal growth factor receptor pathways (GAO *et al.,* 2021). During the regeneration, neurites adjusted their direction and length of growth to the direction of the current as they were parallel to it (MACIAS *et al.,* 2000; HAN *et al.,* 2018). Higher degree of regeneration after reconnection in our study had neurons with a larger dendritic network volume such as Purkinje cells, pyramidal neurons and basal ganglion neurons. The reason for better and faster regeneration of these neurons is stronger coupling effect between them. None of the all

types of cerebellar and cerebellum neurons quantities from the regenerated group have returned to initial values from the control group.

Ultrastructural analysis of components of regenerated rat cerebellum ganglionic neurons showed increased nucleus, disappearance of apoptosis, increased euchromatin relative to heterochromatin in the nucleus, disappearance of nuclear fragmentation and activation of transcription centres in the nucleus. Ganglionic neurons of the cerebellum of rats were reconnected in the regenerated group through re-approaching of their plasma membranes, disappearing of endocytic vesicles, disappearing of microcaveolaes from the interneuron space and normal shape and continuity of plasma membranes has returned. Neuronal regeneration is shown through nuclear brightening, reduction of cytoplasmic vacuolation and the disappearance of microcaveolaes in the plasma membrane (KISHORE *et al.* 2020). HFEMFs have been shown to cause an increase in intracellular calcium levels in neurons (ISAKOVIĆ *et al.,* 2019), the production of new dendrites (PIVOVARENKO, 2019; BAI *et al.,* 2021; GAO *et al.,* 2021) and the regeneration of neuronal perikaryal components (MATHIE *et al.,* 2003; ARENDASH *et al.* 2010). Ultrastructural analysis of the components of regenerated pyramidal neurons of the rat cerebrum showed an increase in nucleus volume, an increase in euchromatin relative to heterochromatin, disappearance of apoptosis, cessation of nucleus fragmentation, restoration of nucleus shape and activation of transcriptional centres in nuclei. Also, there was a reconnection of pyramidal neurons in rat´s cerebrum in the regenerated group through the connecting of plasma membranes of the neurons, reduction of disconnection space, microcaveolaes and endocytic vesicles´ disappearance. Reconnection of pyramidal neurons stimulates their regeneration and restoration of normal functioning. Literature data prove that HFEMF affects not only the plasma membrane, but also membranes of organelles within neurons; especially the mitochondrial and lysosome membranes, by changing their metabolism, (SALFORD *et al.,* 2003). HFEMF improves the work of cytoskeletal components in neurons *in vitro* (AHMAD *et al.,* 2020; KISHORE *et al.,* 2020). The synergistic effect of nerve growth factor (NGF), betamethasone (SENCAR *et al.,* 2020) and HFEMF affects neuronal regeneration and axillary myelination after injury. Damaged neurons receive HFEMF signals via transmembrane receptors and trigger cascade reactions of paracrine hormonal angiogenesis and neurogenesis (LI *et al.,* 2021), stimulate mitochondrial and endoplasmic reticulum (ROMANENKO *et al.,* 2017) and increase neuronal membrane permeability (PÉREZ *et al.,* 2020; ZUO *et al.,* 2023). The greatest importance of our study is in the treatment of Alzheimer's disease with HFEMF because they initiate apoptosis with the aim of removing damaged neurons. Later in the regeneration period, HFEM fields stimulate the process of neuroreparation, neuroregeneration and angiogenesis in order to reconnect the remaining neurons and cure Alzheimer's disease. Authors suggest that accurately controlled HFEMF could have potential therapeutic value, which was the goal of our study.

CONCLUSIONS

Our paper proves the ability of HFEMF to stimulate the reconnection of damaged neurons in the tissues of the cerebrum and cerebellum of rats. The uniqueness of this study lies in the design of the experiment, which was not found in the literature. After two months of rat exposure to HFEMF, one group of them stayed for six months in the environment without these fields. The six-month period is the time in which the nerve tissue of rats was regenerated, and neurons were reconnected. For the first time, the study proves the regeneration and reconnection of nerve cells of the cerebrum and cerebellum with a quantitative stereological unbiased method. Reconnection of individual neurons of the cerebellum and cerebrum was a prerequisite for the coupling effect of nerve tissue regeneration. Nerve cell regeneration is also proven using immunohistochemical staining and analysis of neurons using TEM. Reconnection of neurons

was also possible between those neurons that were already connection before the influence of HFEMF, which is very important for further clinical studies. In the present study, haematological and biochemical analyses proved reversible changes in rat blood parameters after six months of cessation of HFEMF. This conclusion is encouraging, because high-frequency electromagnetic fields do not cause permanent changes in the blood of rats. HFEMF also did not cause allergic reactions in exposed rats, which suggests their safe biomedical use. The exposure time should be determined in accordance with the potential for regeneration of the nervous tissue. This reconnection and regeneration of the nervous tissue in our study gives a chance to restore the functioning of nervous tissue and the organs that innervate it. The frequency of EMFs used to regenerate the affected neural tissues may be fundamentally important to achieve the desired healing effect. In summary the results of the study indicate the potential therapeutic use of HFEMF for the treatment of neuronal CNS dysfunction in humans.

Acknowledgments

Authors thank the Ministry of Scientific and Research Development, Higher Education and Information Society Republic of Srpska, Bosnia and Herzegovina for financial project support (Contract number: 19/6-20/961-98/18).

Ethics committee approval: All animal procedure were in compliance with Directive 2010/63/EU on the protection of animals used for experimental and other scientific purposes and were approved by the Ethical Commitete on Animal Experiments at the Faculty of Mathematics and Science University of Banja Luka, No. 01-9-192.2/19, Bosnia and Herzegovina. The animal health status was monitored daily during the experimnet by the veterinarian trained to work with experimental vertebrates (certificate No. 24-2/2018, Ministry of Agriculture, Forestry and Water Managment Republic of Srpska, BIH).

References:

[1] ACOSTA, S.A., MASHKOURI, S., NWOKOYE, D., LEE, J.Y., BORLONGAN, C.V. (2018): Chronic inflammation and apoptosis propagate in ischemic cerebellum and heart of non-human primates. *Oncotarget* **8** (61): 102820–102834. doi: 10.18632/oncotarget.18330

[2] ADEBAYO, E.A., ADEEYO, A., OGUNDIRAN, M., OLABISI, O. (2019): Bio-physical effects of radiofrequency electromagnetic radiation (RF-EMR) on blood parameters, spermatozoa, liver, kidney and heart of albino rats. *Journal of King Saud University Science* **31** (4): 813–821. doi: 10.1016/j.jksus.2018.11.007

[3] AHMAD, R.H.M.A., FAKHOURY, M., LAWAND, N. (2020). Electromagnetic Field in Alzheimer's Disease: A Literature Review of Recent Preclinical and Clinical Studies. *Current Alzheimer Research* **17** (11): 1001–1012. doi: 10.2174/1567205017666201130085853

[4] AKBARI, H.A., GAEINI, A.A., CHOOBINEH, S. (2020): Moderate exercise training reduced the harmful effects of electromagnetic radiation emitted from a cell phone on hematological parameters in male Wistar rats. *Sport Sciences for Health* **16** (2): 267–272. doi: 10.1007/s11332-019-00600-x

[5] ALGHAMDI, M.S., EL-GHAZALY, N.A. (2012): Effects of Exposure to Electromagnetic Field on of Some Hematological Parameters in Mice. *Open Journal of Medicinal Chemistry* **2** (2) 30–42. doi: 10.4236/ojmc.2012.22005

[6] ARENDASH, G.W., RAMOS, S.J., MORI, T., MAMCARZ, M., LIN, X., RUNFELDT, M., WANG, L., ZHANG, G., SAVA, V., TAN, J., CAO, C. (2010): Electromagnetic field treatment protects

against and reverses cognitive impairment in Alzheimer's disease mice. *Journal of Alzheimer's Disease: JAD.* **19** (1): 191–210. doi: 10.3233/JAD-2010-1228

[7] BAI, W., LI, M., XU, W., ZHANG, M. (2021): Comparison of effects of high- and low-frequency electromagnetic fields on proliferation and differentiation of stem cells. *Neuroscience Letters* **741:** 135-146. doi: 10.1016/j.neulet.2020.135463

[8] BELLOSSI, A., POUVREAU-QUILIEN, V., ROCHER, C., RUELLOUX, M. (1998): Effect of pulsed magnetic fields on triglyceride and cholesterol levels in plasma of rats. *Panminerva Medical* **40** (4): 276–279.

[9] BERZHANSKAYA, J., CHERNYY, N., GLUCKMAN, B.J., SCHIFF, S.J., ASCOLI, A.G. (2013): Modulation of hippocampal rhythms by subthreshold electric fields and network topology. *Journal of Computational Neuroscience* **34**: 369–389. doi: 10.1007/s10827-012-0426-4

[10] BORZOUEISILEH, S., MONFARED, S.A., MORTAZAVI, G.H., ZABIHI, E., POURAMIR, M., SHAFIEE, M., NIKSIRAT, F. (2020): Combined Effects of Radiofrequency Electromagnetic Fields and X-Ray in Renal Tissue and Function. *Research and Reports in Urology* **12**: 527–532. doi: 10.2147/RRU.S257365

[11] DELWATTA, L.S., GUNATILAKE, M., BAUMANS, V., SENEVIRATNE, D.M., DISSANAYAKA, M.L.B., BATAGODA, S.S., UDAGEDARA, A.H., WALPOLA, P.B. (2018): Reference values for selected hematological, biochemical and physiological parameters of Sprague-Dawley rats at the Animal House. *Animal Models and Experimental Medicine* **1** (4) 250–254. doi: 10.1002/ame2.12041

[12] DOGAN, M.S., YAVAS, C., YAVUZ, Y., ERDOGAN, S., YENER, I., SIMSEK, I., AKKUS, Z., ERATILLA, V., TANIK, A., AKDAG, M.Z. (2017): Effect of electromagnetic fields and antioxidants on the trace element content of rat teeth. *Drug Design, Development and Therapy* **11**: 1393–1398. doi: 10.2147/DDDT.S132308

[13] DU, Y., ZOU, Y., YU, W., SHI, R., ZHANG, M., YANG, W., DUAN, J., DENG, Y., WANG, X., LU, Y. (2013): Expression pattern of sorting nexin 25 in temporal lobe epilepsy: A study on patients and pilocarpine-induced rats. *Brain Research* **6** (1509): 79–85. doi: 10.1016/j.brainres.2013.03.005

[14] EL-KAFOURY, B., HAMAM, G.G., EZZAT, S.F. (2019): Effect of Exposure to Different Doses of Cell Phone-Electromagnetic Waves on the Hippocampus and Testis of Adult Albino Rats: A Histological Study. *The Egyptian Journal of Histology* **42** (4): 956–973. doi: 10.21608/ejh.2019.12231.1125

[15] ERTILAV, K., USLUSOV, F., ATAIZI, S., NAZIROĞLO, M. (2018): Long term exposure to cell phone frequencies (900 and 1800 MHz) induces apoptosis, mitochondrial oxidative stress and TRPV1 channel activation in the hippocampus and dorsal root ganglion of rats. *Metabolic Brain Disease* **33** (3): 753–763. doi: 10.1007/s11011-017-0180-4

[16] FABER, D.S., PEREDA, A.E. (2018): Two Forms of Electrical Transmission Between Neurons. *Frontiers in Molecular Neuroscience* **11**. doi: 10.3389/fnmol.2018.00427

[17] FARRUKH, A., FAN, W., ZHAO, S., SALIERNO, M., PAEZ, J., CAMPO, D.A. (2018): Photoactivatable Adhesive Ligands for Light-Guided Neuronal Growth. *ChemBioChem Journal* **19** (8): 1271–1279. doi: 10.1002/cbic.201800118

[18] FLØNES, I.H., VIZARRA, E.F., LYKOURI, M., BRAKEDAL, B., SKEIE, G.O., MILETIĆ, H., LILLENG, P., ALVES, G., TYSNES, B.O., HAUGARVOLL, K., DOLLE, C. (2018): Neuronal complex I deficiency occurs throughout the Parkinson's disease brain, but is not associated with neurodegeneration or mitochondrial DNA damage. *Acta Neuropathologica (Berl.)* **135** (3): 409–425. doi: 10.1007/s00401-017-1794-7

[19] GAO, Q., LEUNG, A., YANG, Y.H., LAU, B.W., WANG, Q., LIAO, Y.L., XIE, J. (2021): Extremely low frequency electromagnetic fields promote cognitive function and hippocampal neurogenesis of rats with cerebral ischemia. *Neural Regeneration Research* **16** (7): 1252-1257. doi: 10.4103/1673-5374.301020

[20] GEMINIANI, A., CASELLATO, C., ANTONIETTI, A., D'ANGELO, D., PEDROCCHI, A.A. (2018): Multiple-Plasticity Spiking Neural Network Embedded in a Closed-Loop Control System to Model Cerebellar Pathologies. *International Journal of Neural Systems* **28** (5): 1750-1771. doi: 10.1142/S0129065717500174

[21] GHADHBAN, F.R., MHEIBES, A. (2018): Study effect electromagnetic field (EMF) and mobile phone radiation on some hematological, biochemical and hormonal parameters in female rats. *Basrah Journal of Veterinary Research* **17** (1): 155–164.

[22] GIKNIS, M.L.A, CLIFFORD, C.B. (2012): Clinical Laboratory Parameter for Crl: Wi (Han) rats. *United States Environmental Protetion Agency.* Available at: https:// www.criver.com/files/pdfs/rms/wistarhan/rm/wistar/han/clin/lab/parameters/08.aspx

[23] HAN, K.S., GUO, C., CHEN, H.C., WITTER, L., OSORNO, T., REGEHR, W.G. (2018): Ephaptic Coupling Promotes Synchronous Firing of Cerebellar Purkinje Cells. *Neuron* **100**: 564-578. doi: 10.1016/j.neuron.2018.09.018

[24] HOSSEINABADI, M.B., KHANJANI, N., SAMAEI, S.E., NAZARKHANI, F. (2019): Effect of long-term occupational exposure to extremely low-frequency electromagnetic fields on proinflammatory cytokine and hematological parameters. *International Journal of Radiation Biology* **95** (11): 1573–1580. doi: 10.1080/09553002.2019.1642542

[25] IACOMINO, M., BALDASSAN, S., TOCHIGI, Y., KOSLA, K., BUFFELLI, F., TORELLA, A., SEVERINO, M., PALADINI, D., MANDARA, L. (2020): Loss of Wox Perturbs Neuronal Migration and Impairs Early Cortical Development. *Frontiers in Neuroscience* **14** (11): 644. doi: 10.3389/fnins.2020.00644

[26] IKONOMIDOU, C., KAINDL, A.M. (2011): Neuronal death and oxidative stress in the developing brain. *Antioxidants and Redox Signaling* **14** (8): 1535–1550. doi: 10.1089/ars. 2010.3581

[27] ISAKOVIĆ, J., GORUP, D., MITREČIĆ, D. (2019): Molecular mechanisms of microglia- and astrocyte-driven neurorestoration triggered by application of electro fields. *Croatian Medical Journal* **60** (2): 127–140. doi: 10.3325/cmj.2019.60.127

[28] KANDEL, M.E., FERNANDES, D., TAYLOR, A.M., SHAKIR, H., POPESCU, C., POPESCU, G. (2017): Three-dimensional intracellular transport in neuron bodies and neurites investigated by label-free dispersion-relation phase spectroscopy. *Cytometry Part a: The Journal of the International Society for Analytical Cytology* **91** (5): 519–526. doi: 10.1002 /cyto.a.23081

[29] KIM, S., IM, W.S., KANG, L. (2008): The application of magnets directs the orientation of neurite outgrowth in cultured human neuronal cells. *Jornal of Neuroscience Methods* **174** (1): 91–96. doi: 10.1016/j.jneumeth.2008.07.005

[30] KIPRIYANOV, A., DOKTOROV, A., PURTOV, P. (2015): Magnetic field effects on bistability and bifurcation phenomena in lipid peroxidation. *Bioelectromagnetics* **36** (7): 485–493. doi: 10.1002/bem.21934

[31] KISHORE, G.K., VENKATESHU, K., SRIDEVI, N. (2019): Effect of 1800-2100 MHz electromagnetic radiation on learning-memory and hippocampal morphology in Swiss albino mice. *Journal of Clinical Diagnostic and Research* **13** (2): AC14-AC17. doi: 10.78 60/JCDR/2019/39681.12630

[32] KISHORE, K., VENKATESHU, K., SRIDEVI, S. (2020): Effect Of 1800-2100 Mhz mobile phone electromagnetic radiation on mice hippocampal Ca3 neurons. *International Journal of Scientific Research World Wide Journals.* **7** (9): 23-35. doi: 10.36106/ijsr

[33] KIVRAK, E.G., ALTUNKAYNAK, B.Z., ALKAN, I., YURT, K.K., KOCAMAN, A., ONGER, E.M. (2017): Effects of 900-MHz radiation on the hippocampus and cerebellum of adult rats and attenuation of such effects by folic acid and Boswellia sacra. *Journal of Microscopy Ultrastructure* **5** (4): 216–224. doi: 10.1016/j.jmau.2017.09.003

[34] KIVRAK, E.G., YURT, K.K., KAPLAN, A.A., ALKAN, I., ALTUN, G. (2017): Effects of electromagnetic fields exposure on the antioxidant defence system. *Journal of Microscopy and Ultrastructure* **5**: 167–176. doi: 10.1016/j.jmau.2017.07.003

[35] LAU, D.H.W., PAILLUSSON, S., HARTOPP, N., RUPAWALA, H., MOROTZ, M., GOMEZ, P.S., GREIG, J., TROAKES, C., NOBLE, W., MILLER, C. (2020): Disruption of endoplasmic reticulum-mitochondria tethering proteins in post-mortem Alzheimer's disease brain. *Neurobiology of Disease*. **143**: 100-120. doi: 10.1016/j.nbd.2020.105020.

[36] LI, W., LIU, W., WANG, W., WANG, J., MA, T., CHEN, J., WU, C., LIU, C. (2021): Sinusoidal electromagnetic fields accelerate bone regeneration by boosting the multifunctionality of bone marrow mesenchymal stem cells. *Stem Cell Research and Therapy* **12** (1): 234-239. doi: 10.1186/s13287-021-02302-z

[37] LIU, G., WANG, T., WANG, T., SONG, W., ZHOU, Z. (2013): Effects of apoptosis-related proteins caspase-3, Bax and Bcl-2 on cerebral ischemia rats. *Biomedical Reports* **1** (6): 861–867. doi: 10.3892/br.2013.153

[38] MAC VICAR, B.A., THOMPSON, R.J. (2010): Non-junction functions of pannexin-1 channels. *Trends Neuroscience* **33**: 93–102. doi: 10.1016/j.tins.2009.11.007

[39] MACIAS, M., BATTOCLETTI, J.H. SUTTON, C., PINTAR, F., MAIMAN, D. (2000): Directed and enhanced neurite growth with pulsed magnetic field stimulation. *Bioelectromagnetics* **21** (4): 272–286.

[40] MATHIE, A., KENNARD, L.E., VEALE, E.L. (2003): Neuronal ion channels and their sensitivity to extremely low frequency weak electric field effects. *Radiation Protection Dosimetry* **106** (4): 311–316. doi: 10.1093/oxfordjournals.rpd.a006365

[41] MESENTIER-LOURO, L.A., TEIXEIRA, C.P., GUBERT, F., VASQUES, J.F., SILVA, A.J.J., ORMONDE, L.C., SANTOS, G.N., OTERO, R.M., SANTIAGO, M.F. (2019): Long-term neuronal survival, regeneration, and transient target reconnection after optic nerve crush and mesenchymal stem cell transplantation. *Stem Cell Research and Therapy* **10** (1): 121. doi: 10.1186/s13287-019-1226-9

[42] NAGAPPAN, P.G., CHEN, H., WANG, D.Y. (2020): Neuroregeneration and plasticity: a review of the physiological mechanisms for achieving functional recovery postinjury. *Military Medical Research* **7** (30). doi: 10.1186/s40779-020-00259-3

[43] NESTOROVIĆ, N., TRIFUNOVIĆ, S., JARIĆ, I., MANOJLOVIĆ-STOJANOVIĆ, M., RISTIĆ, N., FILIPOVIĆ, B., ŠOŠIĆ-JURJEVIĆ, B., MILOŠEVIĆ, V. (2016): Sex steroid application reverses changes in rat castration cells: Unbiased stereological analysis. *Archives of Biological Sciences* **68** (4): 821–828. doi: 10.2298/ABS151201070N

[44] OL'SHEVSKAIA, I., KOZLOV, A.S., PETROV, A.K., ZAPARA, T.A., RATUSHNIAK, A.S. (2009): Influence of terahertz (submillimeter) laser radiation on neurons *in vitro*. *Zhurnal Vysshei Nervnoi Deiatelnosti Imeni and P Pavlova* **59** (3): 353–359.

[45] OLTEAN-DAN, D., GOGARU, G.B., APOSTU, D., MESTER, A., BENEA, H., PAIUSAN, M.G., POPA, C., JIANU, E.M., BODIZS, G.I., BERCE, C., TOADER, A.M., TOMOAIA, G. (2019): Enhancement of bone consolidation using high-frequency pulsed electromagnetic fields

(HF-PEMFs): An experimental study on rats. *Bosnian Journal of Basic Medical Sciences* **19** (2): 201–209. doi: 10.17305/bjbms.2019.3854

[46] OTTO, B.F., THUMM, M. (2020): Nucleophagy – Implications for microautophagy and health. *International Journal of Molecular Science* **21** (12): 4506. doi: 10.3390/ijms21124506

[47] PARAŠ, S., GAJANIN, R., MANOJLOVIĆ, M., RUŽIĆ, Z. (2017): Impact of High-Frequency Electromagnetic Fields on Secretion and Structure of Pancreas in Rats. *Springer Series in Surface Sciences.* **65** (1): 714-721. doi: 10.1007/978-981-10-5122-7_178

[48] PARAŠ, S., TRIŠIĆ, D., MITORVIĆ, A., PROKIĆ, B., DROBNE, D., ŽIVKOVIĆ, S., JOKANOVIĆ, V. (2020): Toxicological Profile of Nanostructured Bone Substitute Based on Hydroxyapatite and Poly(lactide-co-glycolide) after Subchronic Oral Exposure of Rats. *Nanomaterials* **10** (2): 900-918. doi: 10.3390/nano10050918

[49] PASHUT, T., WOLFUS, S., FRIEDMAN, A., LAVIDOR, M., BAR-GAD, I., YESHURUN, Y., KORNGREEN, A. (2011): Mechanism of Magnetic Stimulation of Central Nervous System Neurons. *Computational Biology* **7** (5): doi: 0.1371/journal.pcbi.1002022

[50] PÉREZ, M.J., IVANYUK, D., PANAGIOTAKOPOULOU, V., NAPOLI, G.D., KALB, S., BRUNETTI, D., SHAANA, R.S., KAESER, S.A., FRASCHKA, S., JUCKER, M., ZEVANI, M., VISCOMI, C., DELEIDI, M. (2020): Loss of function of the mitochondrial peptidase PITRM1 induces proteotoxic stress and Alzheimer's disease-like pathology in human cerebral organoids. *Molecular Psychiatry* **26**: 5733–5750. doi: 10.1038/s41380-020-0807-4

[51] PETRIDOU, N., PLENZ, D., SILVA, A.C., BANDETTINI, P. (2009): Direct magnetic resonance detection of neuronal electrical activity. *Proceeding of the National Academy of Sciences* **103** (43): 16015–16020. doi: 10.1073/pnas.060321910

[52] PIVOVARENKO, Y. (2019): Arborization Aqueous Chloride in Pulsed Electromagnetic Fields Justification of Ability to Initiate Formation of Neuronal Dendrites. *International Journal of Neurologic Physical Therapy* **5** (1): 21–29. doi: 10.11648/j.ijnpt.20190501.14

[53] RECORDATI, C., DE MAGLIE, M., MARSELLA, G., MILITE, G., RIGAMONTI, A., PALTRINIERI, S., SCANZIANI, E. (2019): Long-term study on the effects of housing C57BL/6NCrl mice in cages equipped with wireless technology generating extremely low-intensity electromagnetic fields. *Toxicologic Pathology* **47** (5): 598–611. doi: 10.1177/0192623319852353

[54] REES, C.L., WHITE, C.M., ASCOLI, G.A. (2017): Neurochemical Markers in the Mammalian Brain: Structure, Roles in Synaptic Communication, and Pharmacological Relevance. *Current Medicinal Chemistry* **24** (28): 3077–3103. doi: 10.2174/0929867324666170414163506

[55] ROMANENKO, S., BEGLEY, R., HARVEY, A.R., HOOL, L., WALLACE, V.P. (2017): The interaction between electromagnetic fields at megahertz, gigahertz and terahertz frequencies with cells, tissues and organisms: risks and potential. *Journal of the Royal Society, Interface* **137**: 201–207. doi: 10.1098/rsif.2017.0585

[56] RONCAL, TJ., GARCIA, M.F., JIMENEZ, M.E., BAZARRA, N.P., RABANO, A., SAH, N., PRAAG, H., GIACOMINI, D., SCHINDER, F.A., AVILA, J., MARTIN, L.M. (2019): Activity-Dependent Reconnection of Adult-Born Dentate Granule Cells in a Mouse Model of Frontotemporal Dementia. *The Journal of Neuroscience* **39** (29): 5794–5815. doi: 10.1523/JNEUROSCI.2724-18.2019

[57] ROSADO, M.M., SIMKÓ, M., MATTSSON, M.O., PIOLI, C. (2018): Immune-Modulating Perspectives for Low Frequency Electromagnetic Fields in Innate Immunity. *Frontiers in Public Health* **26** (6): 85. doi: 10.3389/fpubh.2018.00085

[58] ROSS, C.L., SYED, I., SMITH, T., HARRISON, B.S. (2017): The regenerative effects of electromagnetic field on spinal cord injury. *Electromagnetic Biology and Medicine* **36** (1): 74–87. doi: 10.3109/15368378.2016.1160408

[59] SALFORD, L.G., BRUN, A.E., EBERHARDT, J.L., MALMGREN, L., PERSSON, B.R.R. (2003): Nerve cell damage in mammalian brain after exposure to microwaves from GSM mobile phones. *Environmental Health Perspectives* **111** (7): 881–883. doi: 10.1289/ehp.6039

[60] SANI, A., LABARAN, M.M., DAYYABU, B. (2018): Effects of Electromagnetic Radiation of Mobile Phones on Hematological and Biochemical Parameters in Male Albino Rats. *European Journal of Experimental Biology* **8** (2).

[61] SANTOS, M., MARCOS, R., SANTOS, N., MALHAO, F., MONTEIRO, R., ROCHA, E. (2009): An unbiased stereological study on subpopulations of rat liver macrophages and on their numerical relation with the hepatocytes and stellate cells. *Journal of Anatomy* **214** (5): 744–751. doi: 10.1111/j.1469-7580.2009.01055.x

[62] SASSE, E.A. (1995): How to define and determine reference intervals in the clinical laboratory approved guideline. *Archives of Pathology and laboratory medicine* **116** (7): 710–3.

[63] SCHNABEL, V., STRUIJK, J.J. (1999): Magnetic and electrical stimulation of undulating nerve fibres: a simulation study. *Medical and Biological Engineering and Computing* **37**: 704–709. doi: 10.1007/BF02513371

[64] SENCAR, L., GUVEN, M., SAKER, D., SAPMAZ, T., TULI, A., POLAR, S. (2020): Ultrastructural effects of nerve growth factor and betamethasone on nerve regeneration after experimental nerve injury. *Ultrastructural Pathology* **44** (4-6): 436–449. doi: 10.1080/01913123.2020.1850965

[65] SHARMA, A., SHRIVASTAVA, S., SHUKLA, S. (2021): Oxidative damage in the liver and brain of the rats exposed to frequency-dependent radiofrequency electromagnetic exposure: biochemical and histopathological evidence. *Free Radical Research* **5** (5) 535–546. doi: 10.1080/10715762.2021.1966001

[66] SHENG, M., SABATINI, B.L., SÜDHOF, T.C. (2012): Synapses and Alzheimer's disease. *Cold Spring Harbor Perspective Biology* **4**. doi: 10.1101/cshperspect.a005777

[67] SHOJAEIFARD, M.B., JARIDEH, S., OWJIFRAD, M., NEMATOLIAHII, S., TALAEI-KHOZANI, T., MALEKZADEH, M. (2018): Electromagnetic fields of mobile phone jammer exposure on blood factors in rats. *Journal of Biomedical Physics and Engineering* **8** (4): 403–408.

[68] SONMEZ, O.F., ODACI, E., BAS, O., KAPLAN, S. (2010): Purkinje cell number decreases in the adult female rat cerebellum following exposure to 900MHz electromagnetic field. *Brain Research* **56**: 95–101. doi: 10.1016/j.brainres.2010.07.103

[69] SURCEL, M., SURCEL, D., TOADER, S., BUTAN, M. (2017): Electromagnetic filed therapy and immune mechanisms which are involved in anti-inflammatory response. *RAD Conference Proceedings.* **2**: 243–248.

[70] TAKEMURA, S., ISONISHI, A., TANAKA, T., OKUDA, H., TATSUMI, K., YAMANO, M., WANAKA, A. (2020a): Neural expression of sorting nexin 25 and its regulation of tyrosine receptor kinase B trafficking. *Brain Structure and Function* **225** (9): 2615–2642. doi: 10.1007/s00429-020-02144-0

[71] TAKEMURA, S., NAGANO, M., ISONISHI, A., TANAKA, T., TATSUMI, K., YAMANO, M., MINAMI, Y., SHIGEYOSI, Y., WANAKA, A. (2020b): Circadian rhythms of sorting nexin 25 in the mouse suprachiasmatic nucleus. *Neurosciences Letter* **14** (727): 134897. doi: 10.1016/j.neulet.2020.134897

[72] TAN, S.Z., TAN, P.C., LUO, L.Q., CHI, Y.L., YANG, Z.L., ZHAO, X.L., ZHAO, L., DONG, J., ZHANG, J. (2019): Exposure Effects of Terahertz Waves on Primary Neurons and Neuron-

like Cells Under Nonthermal Conditions. *Biomedical and Environmental Sciences* **32** (10): 739–754. doi: 10.3967/bes2019.094

[73] TEASDALE, R.D., COLLINS, B.M. (2012): Insights into the PX (phox-homology) domain and SNX (sorting nexin) protein families: structures, functions and roles in disease. *The Biochemical Journal* **441** (1): 39–59. doi: 10.1042/BJ20111226

[74] TEIMORI, F., KHAKI, A.A, HEMMATI, R., RAJABZADEH, A. (2017): Probably Role of Antioxidants Against EMFs-Induced Effects on Central Nervous System Structures. *Crescent Journal of Medical and Biological Sciences* **4** (3): 92–98.

[75] VARGHESE, R., MAJUMDAR, A., KUMAR, G., SHUKLA, A. (2018): Rats exposed to 2.45GHz of non-ionizing radiation exhibit behavioral changes with increased brain expression of apoptotic caspase 3. *Pathophysiology* **25** (1): 19–30. doi: 10.1016/j.pathophys.2017.11.001

[76] WILSON, C.S., MONGIN, A.A. (2019): The signalling role for chloride in the bidirectional communication between neurons and astrocytes. *Neuroscience Letter* **689**: 33–44. doi: 10.1016/j.neulet.2018.01.012

[77] WYSZKOWSKA, J., JANKOWSKA, M., GAS, P. (2019): Electromagnetic Fields and Neurodegenerative Diseases. *Przegląd Elektrotechniczny* **95** (1): 129–133. doi: 10.15199/48.2019.01.33

[78] WYSZKOWSKA, J., JEDRZEJEWSKI, T., PIOTROWSKI, J., WOJCIECHOWSKA, A., STANKIEWICZ, M., KOZAK, W. (2018): Evaluation of the influence of in vivo exposure to extremely low-frequency magnetic fields on the plasma levels of pro-inflammatory cytokines in rats. *International Journal of Radiation Biology* **94**(10): 909–917. doi: 10.1080/09553002.2018.1503428

[79] ZANDI-MEHRAN, N., JAFARI, S., HASHEMI, S., GOLPAYEGANI, F., NAZARIMEHR, N., PERC, M. (2020): Different synaptic connections evoke different firing patterns in neurons subject to an electromagnetic field. *Nonlinear Dynamics* **100** (11): 1809–1824. doi: 10.1007/s11071-020-05576-9

[80] ZHANG, Y., WANG, J., LIU, X., DING, L., WU, X., HE, M., HOU, H., RUAN, G., LAI, J., CHEN, C. (2020): An Investigation into the Effects of Long-Term 50-Hz Power-Frequency Electromagnetic Field Exposure on Hematogram, Blood Chemistry, Fibrosis, and Oxidant Stress Status in the Liver and the Kidney from Sprague–Dawley Rats. *Bioelectromagnetics* **41** (7): 511–525. doi: 10.1002/bem.22291

[81] ZHENG, Y., MA, W., DONG, L., DOU, J., GAO, Y.X.J. (2017): Influence of the on-line ELF-EMF stimulation on the electrophysiological properties of the rat hippocampal CA1 neurons in vitro. *The Review of Scientific Instruments* **88** (10): 105–106. doi: 10.1063/1.5006520

[82] ZUO, H., LIU, X., LI, Y., WANG, D., HAO, Y., YU, C., XU, X., PENG, R., SONG, T. (2023): The mitochondria/ caspase-dependent apoptotic pathway plays a role in the positive effects of a power frequency electromagnetic field on Alzheimer's disease neuronal model. *Journal of Chemical Neuroanatomy* **109**: 101–118. doi: 10.1016/j.jchemneu.2020.101857